# Trabajo Fin de Máster

Máster en Física

# Nanocellular materials from polystyrene nanocomposites by in-situ polymerization


***Autor:***

***Pablo Andrés Romero Proaño***

***Tutor/es:***

***Dr. Miguel Ángel Rodríguez Pérez***

***Dr. Karina Carla Nuñez Carrero***

# Resumen

El uso de nanopartículas en matrices poliméricas ofrece un gran potencial en la mejora de las propiedades mecánicas, térmicas, eléctricas, entre otras de polímeros puros y compuestos convencionales. Sin embargo, para aprovechar al máximo las ventajas de los nanocompuestos, es fundamental lograr una dispersión homogénea de las nanopartículas en la matriz polimérica. En este trabajo, se explora la preparación de nanocompuestos de poliestireno (PS)/sepiolita mediante el proceso de polimerización in situ, con el objetivo de mejorar la dispersión de la sepiolita y su interacción con el polímero. Se utilizó sepiolita sin modificar y sepiolita modificada superficialmente con viniltrietoxisilano (VTES). Durante el proceso de modificación superficial se optimizaron las condiciones de reacción para maximizar la cantidad de grupos silano injertados en la superficie de la sepiolita a traves de la metodología de diseño de experimentos (DoE). Mediante reología dinámica de cizalla se encontró la formación de una red de percolación en los compuestos al agregar 1% en peso de sepiolita sin modificar a la reacción polimerización in situ. A pesar del bajo contenido de sepiolita, la densidad de partículas fue lo suficientemente alta como para formar una red de percolación debido a la excelente dispersión lograda mediante la polimerización in situ. Finalmente, se exploró, inicialmente, la preparación de espumas a partir de estos compuestos. La estructura celular de las espumas se estudió a través de microscopía electrónica de barrido. Se determinó que la modificación superficial de la sepiolita es importante en la generación de estructuras celulares debido a la unión covalente entre el polímero y la carga.



**Palabras clave:** Nanopartículas, polimerización in situ, nanocompuesto, dispersión, sepiolita, poliestireno, red de percolación.

# Abstract

The use of nanoparticles in polymer matrices offers great potential for improving the mechanical, thermal, electrical, and other properties of neat polymers and conventional composites. However, to fully exploit the benefits of nanocomposites, it is essential to achieve a homogeneous dispersion of the nanoparticles in the polymer matrix. This study explores the preparation of polystyrene (PS)/sepiolite nanocomposites through the in situ polymerization process to improve the dispersion of sepiolite and its interaction with the polymer. Both unmodified sepiolite and sepiolite surface-modified with vinyltriethoxysilane (VTES) were employed. The reaction conditions for the surface modification process were optimized to maximize the amount of silane groups grafted onto the sepiolite surface using the design of experiments (DoE) methodology. Dynamic shear rheology revealed the formation of a percolation network in the composites with the addition of 1 wt% unmodified sepiolite during in situ polymerization. Despite the low sepiolite content, the particle density was high enough to form a percolation network due to the excellent dispersion achieved through in situ polymerization. Furthermore, initial exploration was carried out on the preparation of foams from these nanocomposites. The cellular structure of the foams was examined using scanning electron microscopy (SEM). It was determined that the surface modification of sepiolite plays a crucial role in generating cellular structures through the covalent bonding between the polymer and the filler.



**Keywords:** Nanoparticles, in situ polymerization, nanocomposite, dispersion, sepiolite, polystyrene, percolation network.

# Contents

# List of Figures

# List of Tables

# Chapter 1

# Introduction

Polymer nanocomposites (PNCs) are materials composed of a polymer matrix and an inorganic dispersive phase that has at least one dimension in the nanoscale. They have attracted the interest of researchers and industry as a small amount of nanoparticles can provide new or enhanced mechanical, thermal, barrier, optical, and electric properties compared with neat polymers and conventional composites.[1] Since the introduction of the first nanocomposite by Toyota in the 1990s, extensive research has been ongoing to fully exploit the capabilities of these materials.[2] The dispersion and adhesion of nanoparticles within the polymer matrix strongly affect the properties of PNCs. When nanoparticles are uniformly distributed within the polymer matrix, forming a percolation network, the final properties of the material will be enhanced significantly.[3–5] This percolation network refers to an interconnected structure where the nanoparticles are in contact with each other throughout the entirety of the polymeric structure.

Over the past years, several nanomaterials such as graphene[6], carbon nanotubes (CNTs)[7], metallic nanoparticles[8], and nanoclays[9] have been used to enhance polystyrene properties. Nanoclays, in particular, have become popular due to their wide availability, low cost, unique structure, and properties. These minerals include both naturally occurring clays such as montmorillonite, bentonite, and sepiolite, as well as synthetic clays like fluorohectorite and laponite.[10] There is a significant amount of research on lamellar layered silicates, such as montmorillonite and bentonite, which examines the intercalation and exfoliation of the clay on nanocomposites. However, needle-like shape particles such as sepiolite have been less studied even though they present relatively weak interactions and small contact surfaces, which makes the dispersion of fibrous silicates into polymer matrix more uniform.[11]

Sepiolite structure can be seen in Figure 1.1, it presents a fibrous/needle morphology with varying dimensions between 100 and 5000 nm in length, 10-30 nm in width, and 5-10 nm in thickness. It can be represented by the structural formula $Si_{12}Mg_8O_{30}(OH)_4(H_2O)_4 \cdot 8H_2O$, where $4H_2O$ and $8H_2O$ represent coordinated and zeolitic water molecules, respectively.[12] The structure of sepiolite involves the arrangement of two tetrahedral silica sheets surrounding an octahedral sheet made of magnesium oxide-hydroxide as can be seen in Figure 1.1. It allows the presence of small internal and external channels with cross-section dimensions of about 0.36 nm x 1.1 nm that are filled with zeolitic water under ambient conditions. The presence of silanol (Si-OH) groups on the surface of the particles is facilitated by the discontinuity of the silica sheets.[13] The high density of silanol groups ($2.2/nm^2$) are spaced every 0.5 nm along the side of the external channels and enables an ordered availability for coupling reactions with polymers and organic surfactants.[12,14]

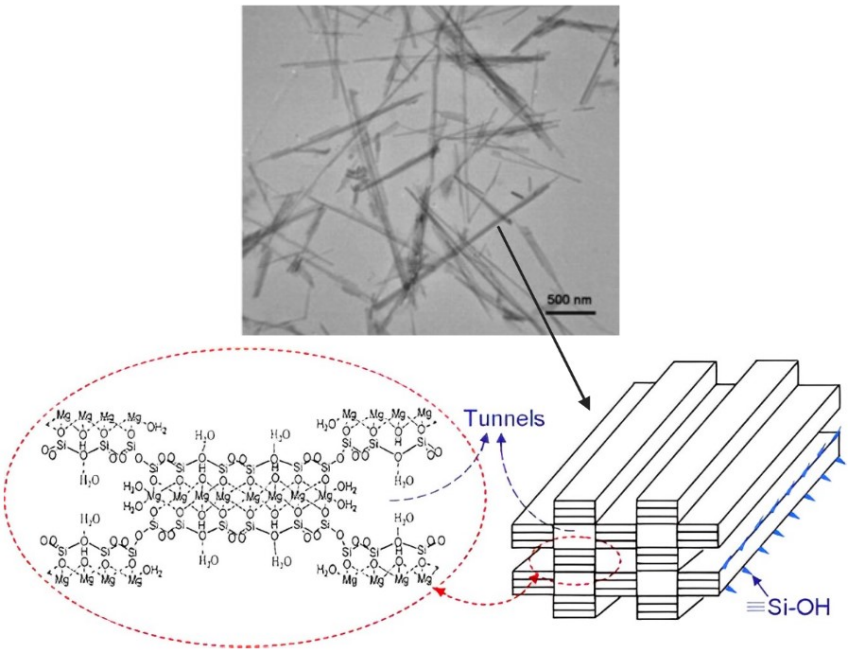


Figure 1.1: TEM image of sepiolite and their corresponding structure diagram. Adapted from [15]

The exceptional sorption and rheological properties and the unique structure of sepiolite account for the improved thermal, mechanical, barrier, and fire retardancy properties of polymer/sepiolite nanocomposites.[11,13] Sepiolite has been used for several applications as adsorbent of heavy metal ions from wastewater, adsorbent of toxic dyes from polluted water, catalyst carrier, immobilization of enzymes, inorganic template to prepare carbon anodes for lithium batteries, preparation of flame retardant and thermal insulation materials, and development of nanocomposites.[16]

Polymer-clay nanocomposites can be synthesized majorly using three techniques including melt blending, solution blending and in situ polymerization.[17] Melt blending technique involves direct mixing of clay particles into the molten polymer matrix. This technique has been the most common commercially implemented technique for PNCs preparation. However, usually issues considering aggregation, phase separation and limited dispersion of the nanoparticles in the polymer matrix are present. Achieving good dispersions in the polymer matrix is difficult via conventional melt processes due to the tendency of these nanoparticles to aggregate into micrometric stacks or bundles driven by van der Waals interactions, ionic interactions, and/or hydrogen bonds.[14,18] The most common techniques used in these cases to improve the compatibility between the filler and the matrix involve the chemical modification of the filler surface and/or the use of compatibilizing agents.[2]

Solution blending consists of dispersing the silicate with a solution of the polymer in an organic solvent, followed by evaporation of the solvent or precipitation of the polymer. The main disadvantage of this technique is the need to use large amounts of solvents and the necessity for the matrix to be readily soluble in the solvent.[2]

During the in situ polymerization process, the nanoparticles are incorporated into the polymer matrix while the polymer is being synthesized. The process takes place when the polymer chains grow from the particle's surface or through conventional radical polymerization, which can be combined with dispersion,

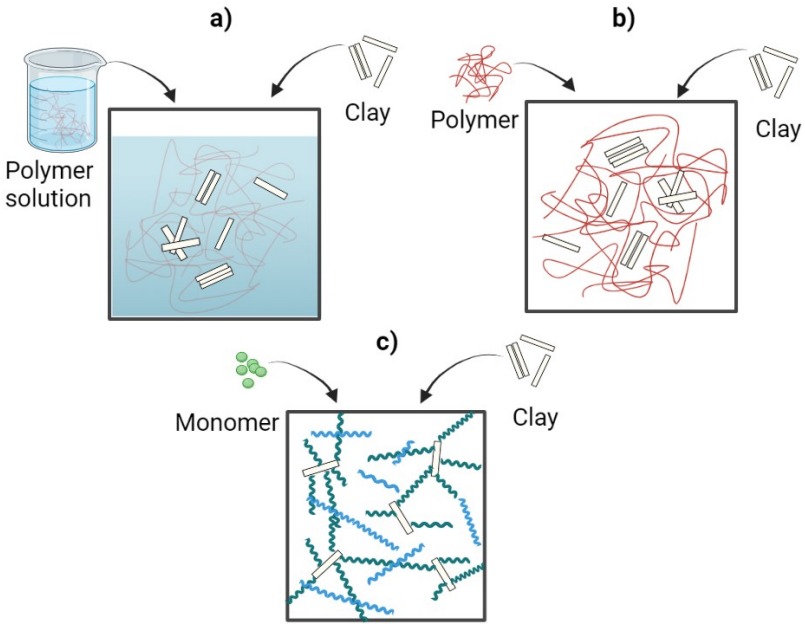


Figure 1.2: Schematic representation of clay nanocomposite preparation methods. a) Solution blending, b) melt blending and c) in situ polymerization.

suspension and emulsion polymerization methods.[14] In situ polymerization allows better control over the dispersion of nanoparticles and results in a more well-defined structure of the nanocomposites.[18] In addition, this technique improves the interaction between the matrix and the filler. In literature, comparative studies between in situ polymerization and melt blending prepared polymer-sepiolite nanocomposites can be found. Herrero et al.[19] prepared bio-based polyamide 11/sepiolite nanocomposites and found that the nanocomposites obtained by in situ polymerization presented higher values of Young modulus, tensile strength, and heat distortion temperature due to a better dispersion of the nanoclay in the final composites. Similarly, Nair et al.[20] found that high-impact polystyrene/vinyl clay nanocomposites present a better dispersion of the clay in the matrix and give better properties when in situ polymerization method is used.

Polystyrene is a synthetic aromatic polymer made from styrene monomer, and it is one of the most widely employed thermoplastics today. Amorphous or general-purpose polystyrene is colorless, transparent, stiff, hard and has outstanding electrical resistance and low dielectric loss.[21] It is used in applications and sectors such as: packaging, toys, appliances, furniture industry, automotive pieces, building insulation, among others. Moreover, polystyrene copolymers and foams, which include high-impact polystyrene (HIPS) containing 5-8 % butadiene and expandable polystyrene (EPS), represent a large percentage of the total consumption of polystyrene.

The proper interaction through a uniform distribution of sepiolite in the polystyrene matrix plays a key role in improving the performance of PNCs. However, because of their hydrophilic properties, silicate minerals such as sepiolite lack affinity for hydrophobic organic polymers. This leads to an inhomogeneous distribution and an extended phase separation between nanoparticles in the polystyrene matrix. In order to address this problem, surface modification of sepiolite according to the polarity of the system reduces its surface energy and enhances its miscibility within the polymer matrix. Among the modification methods, the use of organosilanes is a simple way to introduce functional groups onto the surface of sepiolite and

other inorganic particles.[14]

Organosilanes present both organic functional groups and alkoxy or halo groups in one molecule. The hydrolyzable alkoxy or halo groups are covalently bonded onto sepiolite via condensation through the silanol groups on the sepiolite surface. Moreover, the functional group allows the conjugation of the silane molecule to other functional organic compounds, such as hydrophobic polymers.[22] After the modification reaction, the grafted silane groups on the sepiolite surface are very stable and are eliminated only by burning.[14] Several factors, including solvents, pH, temperature, silane concentration, surface hydration, type of organosilane affect the way silane-derivatized molecules interact with the substrate.[23] These factors influence the efficiency of grafting or covalent bonding of silane molecules on sepiolite surface. The surface modification of sepiolites with organosilanes is frequently performed in a mixture of water/alcohol (mostly ethanol or isopropanol) but also in toluene, water, or anhydrous solvents.[11,24] The choice of solvent is crucial as sepiolite can disperse well in polar solvents and build a colloidal network structure. A good dispersion in the solvent allows the surface modification on individualized sepiolite fibers instead of just the external surface of sepiolite aggregates.[24]

Also, the interactions between other reactions conditions such as pH, time, temperature, and silane concentration influences the silanization process, affecting the final degree of grafting and dispersibility of sepiolite. Among the different studies that have performed a silanization process of sepiolite for nanocomposite applications it is possible to find many differences in the reactions conditions used, even for the same organosilane. For example, with isopropanol as a solvent, Rehman et al.[25] used vinyltriethoxysilane (VTES) to modify sepiolite using a reaction time of 24 hours, an acidic pH, a silane ratio of 2.4 ml per gram of sepiolite, and room temperature. With the modified sepiolite, they prepared polystyrene/sepiolite clay nanocomposites via the melt extrusion technique. Masood et al.[26] prepared flame retardant ethylene-vinyl acetate (EVA) nanocomposites by melt blending. For this, they modified sepiolite with vinyltrimethoxysilane (VTMS) using a neutral pH, a reaction time of 24 hours, a silane ratio of 2.06 ml per gram of sepiolite and a temperature of 60 $^oC$. Ajmal et al.[27] prepared nanocomposites of poly-3-hydroxybutyrate-co-3-hydroxyvalerate (PHBV) and vinyltriethoxysilane grafted sepiolite by solution casting. In this case, the reaction conditions on the sepiolite surface modification were: neutral pH, reaction time of 2 hours, silane ratio of 1.2 ml per gram of sepiolite and room temperature.

In this context, part of this work focuses on the study of pH, time, temperature, and silane concentration effects in the silane grafting reaction. Then, design of experiments (DOE) methodology is used to study the influence of the reaction conditions on the silane grafting degree onto sepiolite surface and to optimizate the process for maximizing the silane grafting. DoE is a technique used to strategically plan experiments about multivariable problems with few attempts and analyze the resulting data.[28] It involves conducting a series of tests where intentional modifications are made to the input variables of a process, allowing for the identification of factors responsible for changes in the desired output response and to find an optimum for the process. By analyzing the collected data, a mathematical model of the studied process is constructed. Through DoE, we gain insights into how specific factors impact the variables of interest, enabling us to draw valid and objective conclusions.[29]

It is important to mention that organosilanes with a vinyl functional group are used in this work during the surfcae modification process due to their reactivity with styrene monomers. In this way, the polymerizable vinyl groups allow the initiation and propagation of polystyrene chains to form polymer

brushes on the sepiolite surface.[30] The chemical structure of vinyltriethoxysilane (VTES) used to improve the dispersion and compatibility of sepiolite with a polystyrene matrix can be seen in Figure 1.3.

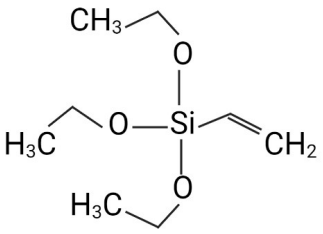


Figure 1.3: Chemical structure of vinyltriethoxysilane (VTES) used in this work.

Among the few works about polystyrene/sepiolite nanocomposites or nanohybrids, it is possible to find melt extrusion[13,25], radiation-induced graft polymerization[31] and emulsion graft polymerization[32] as preparation methods. Polystyrene/sepiolite nanocomposites using vinyltriethoxysilane (VTES) as the compatibilizer and cross-linking agent via melt extrusion technique have been studied by Rehman et al.[25] They found that the incorporation of 4 wt.% sepiolites caused an increase of 15 % in the tensile strength and 25 % in Young's modulus of polystyrene nanocomposites. Also, the flame retardancy of the nanocomposite was enhanced compared to the pure polymer. Shaista et al.[31] synthesized polystyrene grafted sepiolite nanohybrid by using a simultaneous radiation grafting technique in the presence of dichloromethane (DCM) as solvent. As indicated by them, the grafting yield increased with the assimilated portion, and the system allowed for controlled grafting of styrene onto sepiolite in dichloromethane. The use of sepiolite in polystyrene for magneto-optical Faraday activity in straightforward FeCo-sepiolite/polystyrene nanocomposites was explored by Fernandez et al.[33] By melt compounding process, they obtained transparent composites with high magnetic susceptibility. Within the CellMat research group, Ballesteros et al.[13] obtained blends of polystyrene with sepiolites using a melt extrusion process to prepare polymerics foams. They obtained a percolated network when using 6.0 wt % of quaternary ammonium modified sepiolite, 8.0 wt % of natural sepiolite and 10.0 wt % of organo-modified sepiolite.

Within this framework, this work aims to improve the dispersion of sepiolite in PS/sepiolite nanocomposites by using in situ suspension polymerization technique. The incorporation of well-dispersed sepiolite in the polystyrene matrix can enhance the structural, thermal and rheological properties of the nanocomposites that later can be used in the preparation of cellular materials.

A cellular material is composed of two well differentiated phases: a dispersed gaseous phase within a continuous solid matrix. The ones whose solid structure is given by a polymeric matrix are known as polymeric cellular materials or polymeric foams. These foams find extensive applications due to their lightweight nature and affordability. Moreover, they serve as excellent example of a tailored material, as they can be modified to have the desired mechanical and thermal properties by adjusting the expansion grade related to the foam density, or by the inclusion of additional phases in the polymeric matrix, as micro or nanofillers.[34] Cellular materials can exhibit varying degrees of interconnectivity within their cellular structures. Open-cell materials are characterized by the presence of the polymeric phase present only in the cell edges, also referred to as struts. In contrast, closed-cell materials have the polymer present in both the struts and the cell walls.[35]

The foaming mechanisms affecting the cellular structure of a material are nucleation, cell growth,

degeneration and stabilization. The first one refers to the generation of small bubbles, or nucleus in the material in the presence of a gaseous phase. Nucleation occurs as a result of thermodynamic instability caused by factors such as temperature increase or pressure release. When a secondary phase, such as sepiolite particles, acts as preferred nucleation sites, it is referred to as heterogeneous nucleation. The equation governing heterogeneous nucleation is expressed as follows:[3]

$$N_{het} = C_1 f_1 exp\left(\frac{- \triangle G'_{het}}{kT}\right) \tag{1.1}$$

Where $C_1$ represents the initial concentration of gas in the polymer matrix, $f_1$ is the frequency factor of the gas molecules, k is the Boltzmann constant, T is the temperature, and $\triangle G'_{het}$ is the free energy barrier associated with heterogeneous nucleation. This barrier must be surpassed to achieve the formation of a stable nucleus. During the cell growth stage, energy is provided to the system to facilitate the growth of the formed nucleus into fully formed cells. In the later stages of cell growth, various degeneration mechanisms can occur. If they are not properly controlled, they can deteriorate the cellular structure. Finally, it is necessary to stabilize the structure as the gas escapes through the thin walls, and cells may collapse, resulting in foam contraction. Stabilization in thermoplastic materials involves rapidly cooling the sample to a temperature below the effective glass transition temperature, particularly in the case of amorphous polymers.[3]

Cellular nanocomposites refer to foams that are produced from polymer nanocomposites. In addition to improving the morphology and properties of the solid polymer matrix, nanoparticles have the ability to alter the characteristics of the cellular structure.[36] When present in small quantities and well-dispersed, nanoparticles act as heterogeneous nucleation sites, thereby modifying the cellular structure and leading to lower cell sizes and higher cell nucleation densities.[37] Moreover, nanoparticles can influence the extensional rheological properties of the polymer matrix, which play a crucial role in degeneration mechanisms. This, in turn, affects the cell size, homogeneity of the cellular structure, and foam density.[36]

Polystyrene (PS) foams rank as the second largest component in the foam market after polyurethane (PU) foams.[3] Various particles such as montmorillonites, silica, and nano-porous silica have been widely used to produce cellular PS based composites.[36] There are few studies about the use of sepiolites to modify the cellular structure of PS foams. Notario et al.[38] reported that the addition of just 0.5 wt% of sepiolites can reduce the cell size of PS foams by 60%. Ballesteros et al.[39] conducted a more comprehensive study about how the dispersion degree of sepiolite particles and the extensional rheological behavior of the solid polymer composite affect the cellular structure of the foams. They found that the introduction of a higher percentage of sepiolites resulted in an increase in the open cell content. Moreover, using sepiolites modified with quaternary ammonium salts at a concentration of only 2 wt% led to a substantial 82% reduction in cell size compared to pure PS.

In the previously mentioned studies, the foaming process was carried out from PS/sepiolite nanocomposites obtained from the melt blending method. However, the formation of PS/sepiolite foams through in situ polymerized nanocomposites has not been investigated. The advantages of in situ polymerization in the dispersion and compatibility of sepiolite in the polystyrene matrix might contribute to the creation of a uniform cellular structure with higher cell nucleation density and smaller cell sizes during the foaming process. As a result, the final phase of this research aims to investigate the impact of nanocomposites obtained through in situ polymerization on the generation of cellular structures.

# Chapter 2

# Objectives

The primary goal of this work is to study the influence of in situ suspension polymerization technique in the dispersion of sepiolite in a polystyrene matrix. For this purpose, pristine and surface modified sepiolite with organosilanes containing vinyl or allyl groups will be used. Moreover, this work intends to study the generation of cellular structures from the obtained nanocomposites.

To achieve this objective, it is necessary to accomplish the following steps:

- Study the influence and effects of reaction conditions such as pH, time, temperature, and silane concentration in the silane grafting amount on sepiolite surface through the design of experiments (DoE) methodology.
- Analyze the effect of the addition of unmodified/modified sepiolite in the polystyrene matrix during the in situ polymerization reaction.
- Characterize the composites obtained by in situ polymerization method focusing on their structural, thermal and rheological properties.
- Prepare foams employing the gas dissolution foaming method from the previously obtained PS/sepiolite nanocomposites.
- Determine the effects of varying the amount of filler in the structure of the prepared composites and foams.

# Chapter 3

# Methodology

## 3.1 Chemicals and materials

Sepiolite (UNV-1) was supplied by Tolsa. For the surface modification process vinyltriethoxysilane (VTES; 97%; $M_w$ = 190.31), hydrochloric acid (HCl) 35 %, and 2-Propanol solvent ($(CH_3)_2CHOH$) ≥ 99.8% (GC) were used, they were provided by Sigma-Aldrich, Scharlau and Honeywell, respectively. During the in situ polymerization styrene, 2,2'-Azobis(2 methylpropionitrile) (AIBN), polyvinyl alcohol (PVOH; $M_w$ 85,000-124,000 and 87-89% hydrolysed), and methanol (MeOH) were used and provided by Sigma-Aldrich.

## 3.2 DoEs methodology

The experiments were conducted following the full factorial design approach, which involves exploring all possible combinations of different factor levels to gather information about their main effects.[29] The statistical software Minitab was used to generate DoEs and analyze the collected data.

The silanization reaction conditions, including pH, temperature, time, and silane concentration were considered as independent variables, while the silane grafting percentage was treated as the dependent variable or response parameter. The first DoE consisted of two factors with 2 levels and two factors with 3 levels, giving a total of 36 experimental runs. The factors and their corresponding levels for this DoE are presented in Table 3.1. The second DoE used a $3^2$ full factorial design which factors and levels are presented in Table 3.1. To eliminate bias in measurements, all experiments were conducted randomly. The resulting combination of experiments in both DoEs can be found in Annexes section.

## 3.3 Sepiolite silanization reaction

The surface modification procedure followed in the DoEs started by suspending 2.5 g of sepiolite in 50 ml of 2-propanol/water mixture (90:10 w/w) using a round bottom flask. Then, the necessary amount of HCl was added, and the solution was stirred for 10 minutes. Afterward, the necessary amount of organosilane was added and stirred under these conditions for 4 or 24 hours. Experiments carried out at 60 $^oC$ used a silicone bath under reflux conditions. The modified sepiolite was filtered and washed thrice

Table 3.1: First and second DoE factors with their corresponding levels used to study the grafting reaction of VTES molecules on sepiolite surface.

| DoE | Factors | Levels | Values |
|---|---|---|---|
| **1** | **A** Acid amount | 3 | No acid<br>0.1 ml<br>2 ml |
| | **B** Temperature | 2 | 25 $^oC$<br>60 $^oC$ |
| | **C** Time | 2 | 4 h<br>24h |
| | **D** Silane concentration | 3 | 0.25 ml/g of sepiolite<br>0.8 ml/g of sepiolite<br>2.4 ml/g of sepiolite |
| **2** | **A** Acid amount | 3 | 0.1 ml<br>0.8 ml<br>1.5 ml |
| | **B** Silane concentration | 3 | 1.6 ml/g of sepiolite<br>2.4 ml/g of sepiolite<br>3.2 ml/g of sepiolite |

with distilled water and once with 2-propanol to remove unreacted silane and HCl. Finally, the product was dried in a vacuum oven at 300 mbar and 60 $^oC$ for 24 hours.

After the DoE 1 and DoE 2 analysis, the silanization process was optimized to obtain the maximum silane grafting amount for using the modified sepiolites to prepare polystyrene/sepiolite nanocomposites. For this, a solution of 2-propanol (50 ml) and sepiolite (2.5 g) was previously sonicated for 30 minutes to enhance its dispersion in this solvent. Then, the surface modification reaction with vinyltriethoxysilane and allyltriethoxysilane was carried out following the procedure described previously with 0.8 ml HCl, 8 ml of silane, a temperature of 60 $^oC$ and a reaction time of 24 hours.

## 3.4 Nanocomposites in situ polymerization

### 3.4.1 Suspension polymerization

In a 100 mL two-neck flask were placed 40 mL of distilled de-ionized (DDI) $H_2O$, 0.4 g of PVOH (1 g PVOH / dL $H_2O$) and sepiolite. The mixture was heated and stirred under nitrogen atmosphere until a solution was formed. In a separate flask was placed 12 mL of styrene and 0.086 g of AIBN ($5x10^{-3}$ mol AIBN / mol styrene). The mixture was deoxygenated with $N_2$ (g) and stirred until a solution was obtained and keeping it cold at 0 $^oC$. This organic solution was added dropwise to the aqueous system, and it was kept under inert atmosphere at 64 $^oC$ with constant stirring during 24 h. Completing the polymerization, the reaction mixture was kept cooled to promote stabilization of the polystyrene (PS) particles. Finally, the PS particles were separated by centrifugation (10.000 rpm) and washed repetitively with hot water

and methanol. The polymer was air-dried and then dried at reduced pressure for 48 h at 80 $^oC$.

## 3.5 Gas dissolution foaming process

Before the foaming process, the neat PS and different composites obtained from the in situ polymerization process were thermoformed in a hot plate press to obtain circular plates with 25 mm in diameter and 2 mm in width. The compression molding process was performed at a temperature of 170 $^oC$. The foaming of the samples was achieved using the solid-state gas dissolution foaming method. For this purpose, a high-pressure vessel (model PARR 4681) provided by Parr Instrument Company has been used. The material foaming process under the different stages can be seen in Figure 3.1.

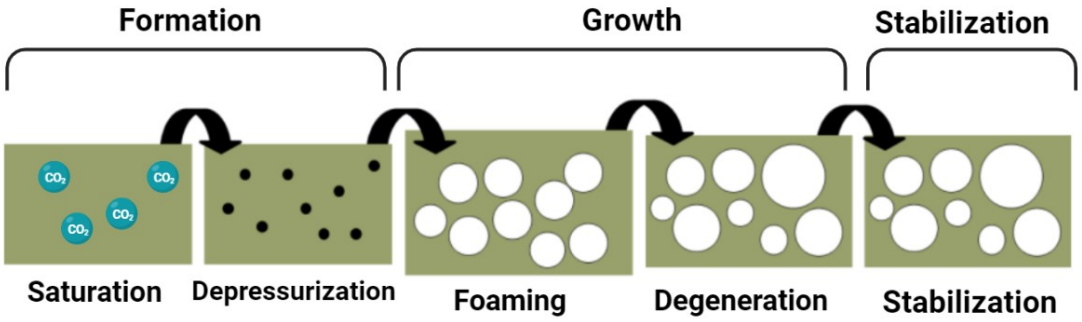


Figure 3.1: Schematic representation of cellular materials formation under gas dissolution foaming process. Adapted from[40]

The initial step of the gas foaming process was the saturation step. In this stage, the samples were placed in the high-pressure vessel, and carbon dioxide ($CO_2$) gas was introduced at a saturation pressure ($P_{sat}$) of 8 MPa and a saturation temperature ($T_{sat}$) of 40 $^oC$ for 24 hours. When the material was placed in the autoclave under these conditions, gas diffusion inside the material started to take place, and $CO_2$ filled the empty spaces between the polymer chains, resulting in reduced viscosity and a lower $T_g$ of PS.[3]

The next part of the process was the depressurization stage, during which the gas pressure was released. The abrupt decrease in pressure creates a thermodynamic instability that can trigger a nucleation process, which leads to the formation of small nuclei as the solid and gaseous phases separate.[41] In this work, as a two-step gas dissolution foaming method was employed for the foaming stage, samples were immersed in a silicone bath at 120 $^oC$ for a duration of 1 minute. By maintaining the foaming temperature above the effective glass transition temperature, the polymer remains in a rubbery state, allowing the polymeric chains to have sufficient mobility. This mobility enables the nucleation points to start to grow, creating the final cells of the cellular structure.[3] The time between the pressure release and immersion in the thermal baths was approximately 2 minutes. Once the materials expanded, they were rapidly cooled in water to stabilize the cellular structure and minimize degeneration mechanisms.

## 3.6 Characterization

### 3.6.1 Thermogravimetric analysis (TGA)

Thermogravimetric analysis (TGA) is an analytical method employed to assess the thermal stability of a material and determine the proportion of volatile components present by monitoring the weight variation during controlled heating.[42] By subjecting the sample to a specific heating protocol, TGA allows the investigation of mass changes linked to both physical and chemical transformations.

TGA was used to evaluate the thermal degradation of sepiolite and estimate the organic modifier amount on sepiolite surface from the volatilized mass between 350 and 650 $^oC$. Also, with this method it has been possible to study the thermal stability of the synthesized nanocomposites and characterize the final amount of clay present in them. The analysis was carried out using a Mettler Toledo TGA/DSC $3^+$, where around 10 mg of each sample in alumina crucibles were used. The measurements of the modified sepiolites were carried out under nitrogen atmosphere from room 50 to 1000 $^oC$, with a heating rate of 20 $^oC$/min. In the case of polystyrene/sepiolite nanocomposites, the heating range was from 50 to 850 $^oC$.

### 3.6.2 Differential scanning calorimetry (DSC)

Differential scanning calorimetry (DSC) is a technique that measures the heat flow difference between a sample and a reference as a function of temperature. It allows for the quantification of the energy involved in each transition that a polymer undergoes during a heating protocol.

The glass transition temperature ($T_g$) of the synthesized polystyrene and polystyrene/sepiolite nanocomposites were determined using this technique. The analysis was carried out using a Mettler Toledo DSC $3^+$ equipment. The samples were heated from 20 to 160 $^oC$ at a heating rate of 10 $^oC$/min under nitrogen atmosphere. Once the temperature reached 160 $^oC$, it was maintained for 3 minutes before cooling back down to 20 $^oC$. Then, the heating cycle was repeated and only the results of the second scan were reported to avoid the influence of the thermal history of the sample.

### 3.6.3 Fourier transform infrared spectroscopy (FTIR)

Fourier transform infrared spectroscopy (FTIR) technique relies on detecting the specific vibrations of functional groups in molecules when they are exposed to certain wavelengths of light. These vibrations, along with their intensity (% transmission or absorbance), are plotted against the frequency of light ($cm^{-1}$) to generate an FTIR spectrum. This enables the qualitative identification of the present species by examining the characteristic bands in the sample's spectrum, providing valuable information about the sample's chemical composition.[43]

FTIR is used in this work to identify the covalent bonding between silane molecules and silanol groups on sepiolite surface. Also, it is used to study the interactions between polystyrene and modified sepiolite in the nanocomposite samples. The spectra were performed using a Bruker Tensor 27 spectrometer in the range of 4000-600 $cm^{-1}$.

### 3.6.4 Gel permeation chromatography (GPC)

Gel permeation chromatography (GPC) is a widely employed method for characterizing polymers, providing information about their molecular weight distribution and polydispersity. GPC achieves separation of polymer molecules based on their hydrodynamic volume by employing columns with varying porosity. The output from the columns is then analyzed using one or more detectors that are typically calibrated with linear polymer standards.[44]

This technique is used in this work to determine the number- and weight-average molar mass ($M_n$, $M_w$) and dispersity (Đ) of the synthesized polystyrene and polystyrene/sepiolite nanocomposites. Also, the influence of unmodified/modified sepiolite on the resulting nanocomposites molecular weight distribution is going to be studied. The analysis was carried out using a Waters HPLC 515 pump, injector and a Waters 410 refractometer. Samples are passed through 1 precolumn and an Agilent column at $35^oC$ using chloroform as solvent at a flow rate of 0.5 mL/min.

### 3.6.5 Rheological tests

Rheological characterization involves studying how materials flow and deform when subjected to external forces, which are determined by their internal structure and molecular interactions and provide valuable insights into their behavior and properties. In oscillatory shear tests, the sample is placed between two plates; while the lower plate is fixed, the upper plate oscillates with a certain frequency of oscillation ($\omega$). From a rheological point of view, polymers are defined as viscoelastic materials, which means that they present a behavior between an ideal solid elastic and an ideal Newtonian fluid.[45]

The viscoelastic properties that can be studied through dynamic shear rheology include the storage modulus (G'), the loss modulus (G"), and the tangent of the phase angle ($\delta$), which are examined in relation to variables such as time, frequency, temperature, and material deformation. G' provides insights into the material's elastic component, indicating its ability to recover its original shape under applied stresses.[46] On the other hand, G" tells us about polymer's ability to dissipate energy, with part of the energy being used to change the structure of the material during flow, and the rest of this energy is spent in heating the material. The phase angle ($\delta$) also provides information about a material's damping characteristics. In the case of a viscoelastic material (such as polymers), the phase angle varies between $0^o$ and $90^o$, which means that the stress shows a certain delay period compared to the strain curve.[3] The equations that represent the storage modulus, loss modulus and phase angle are the following:

$$G' = \frac{\sigma_0}{\gamma_0} cos\delta \tag{3.1}$$

$$G'' = \frac{\sigma_0}{\gamma_0} sin\delta \tag{3.2}$$

$$tan\delta = \frac{G''}{G'} \tag{3.3}$$

Where $\sigma_0$ is the stress amplitude and $\gamma_0$ is the strain amplitude.

Figure 3.2 shows the typical rheological behavior of a polymer in relation to frequency. At high frequencies, the storage modulus is higher than the loss modulus, indicating the glassy region. As the frequency decreases, the mobility of the polymer chains increases, leading to a transition to the rubbery plateau where the material exhibits predominantly elastic behavior. The region between the glassy state

and the rubbery plateau is known as the transition region or $T_g$ region, where the loss modulus reaches its maximum value. This behavior arises from the energy required to enhance the mobility of the polymer chains. At very low frequencies, the terminal flow region is reached, characterized by a higher viscous modulus compared to the elastic modulus. In this region, the viscosity remains constant. In this work, the regions of interest that are going to be analyzed are the rubbery plateau and the terminal flow region. In this frequency range, it is possible to see that the loss modulus and storage modulus curves intersect at a specific frequency, known as the cross-over frequency ($\omega_x$).[3]

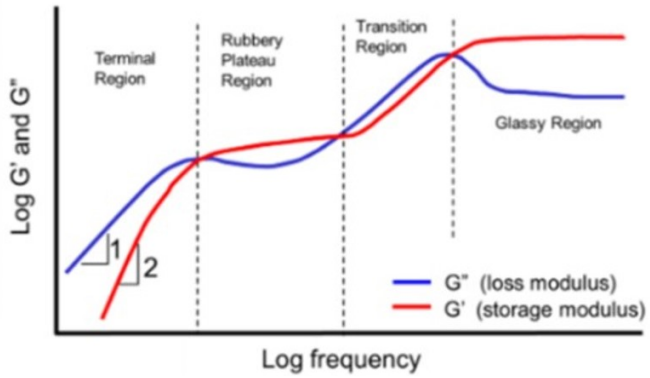


Figure 3.2: Rheological behavior of a polymer plots showing their characteristic regions in Log G' and G" as a function of the frequency curves. Adapted from[3].

In this work, dynamic shear rheology technique was used to evaluate the dispersion degree of the neat PS and the different nanocomposites. The measurements were performed in a shear stress-controlled rheometer (AR 2000 EX from TA Instruments) at a temperature of $220^oC$, under a nitrogen atmosphere, and using 25 mm diameter parallel plates. To determine the linear viscoelastic region of the nanocomposites, a strain sweep test was performed at a fixed dynamic frequency of 1 rad/s. To analyze G', G" and complex viscosity values a frequency sweep was performed covering a range of angular frequencies from 0.2 and 100 rad/s, considering that lower temperatures led to sample degradation.

### 3.6.6 X-ray radiography

The interaction between X-rays and matter is linked to the complex refractive index ($n$) of the materials involved, wherein the real and imaginary components play a significant role in phase and absorption contrast, respectively[40]. An X-ray radiography image obtained by exposing a material to X-rays provides a shadow of intervening structures that directly depend on the material's density ($\sigma$) and atomic number ($Z$).[47] Thus, the resulting image is formed based on the quantity and intensity of X-rays detected at each point. The experimental setup used to obtain the radiography images can be seen in Figure 3.3.

In this study, X-ray radiography is employed to evaluate the dispersion and distribution of sepiolite in the polystyrene matrix at a high-size scale. In this specific case, sepiolite aggregates that were formed due to the high concentration of silane used during the surface modification process can be analyzed with this technique. The basic elements of the radiography setup used in this work include a low energy microfocus X-ray source (L10101, Hamamatsu. Voltage: 20-100 kV, Current: 0-200 $\mu A$) and a high sensitivity flat detector panel which forms the X-ray images (C7940DK-02, Hamamatsu. 2240 x 2344

pixels, 50 $\mu m$ pixel size). Both elements are positioned at a source-to-detector distance (SDD) of 580 mm.

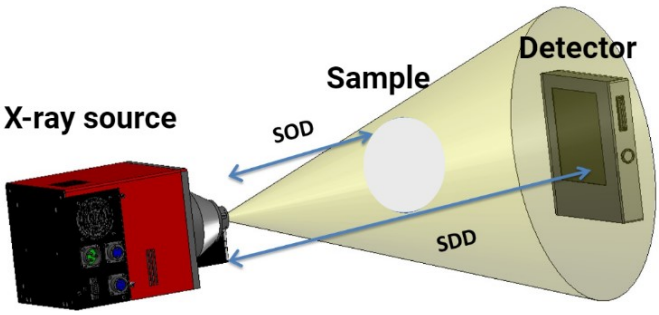


Figure 3.3: 3D diagram of the setup employed to perform the X-ray radiography measurements showing the relative position of the sample with respect to the X-ray source and detector. Adapted from[48].

### 3.6.7 Density measurements

The density of the foamed materials ($\rho_f$) was measured using the water displacement method, which is based on Archimedes' principle and follows the ISO 1183-1 standard. For this, a density determination kit for the balance Mettler Toledo AT261 was used.

The relative density and expansion ratio were calculated using the foam density and the density of the solid PS sample ($\rho_s$). The relative density ($\rho_r$) is obtained as the reciprocal of the relative density. Similarly, the expansion ratio is defined as the ratio between the density of the cellular material and $\rho_s$.[3]

$$\rho_r = \frac{\rho_f}{\rho_s} \tag{3.4}$$

$$Er = \frac{1}{\rho_r} \tag{3.5}$$

### 3.6.8 Scanning electron microscopy (SEM)

Scanning electron microscopy (SEM) is a technique that uses a electron beam directed towards the material, scanning its surface. As the beam interacts with and penetrates the material, various interactions take place, resulting in the emission of photons and electrons from the sample surface or its vicinity. To generate an image, the signals produced by the electron-sample interactions are detected using different types of detectors, which depend on the specific mode of SEM being employed.[49]

The cellular size of the different foams prepared by gas dissolution foaming process was estimated using SEM images. From the cell size values, the cell nucleation density of the foams was calculated by using the following formula:

$$N_o = \frac{6}{\pi\phi^3}(\frac{1}{\rho_r} - 1) \tag{3.6}$$

Where, $\phi$ is the cell size and $\rho_r$ is the relative density of the foams.

The measurements were performed in a Flex SEM 1000 from Hitachi. Prior to being placed in the SEM, the solid samples were cooled in liquid nitrogen, fractured, and coated with a thin layer of gold to ensure electrical conductivity.

# Chapter 4

# Results & Discussion

## 4.1 Sepiolite surface modification

The reaction mechanism of the surface modification of sepiolite starts with the hydrolysis of the ethoxy groups from vinyltriethoxysilane (VTES) or allyltriethoxysilane (ATES). As we use sepiolite conserved in normal conditions after drying, it leads to the presence of zeolitic water. Then, the hydrolysis reaction can be favored from this water and from water added to the reaction. The resulting silanol groups may interact with the sepiolite Si-OH groups and/or condense to form siloxane bonds.[23] In this sense, sepiolite surface silanols serve as nucleation sites for the favorable hydrolysis and condensation of organosilanes during the reaction period.[24] The scheme of the reaction mechanism in the presence of VTES can be seen in Figure 4.1.

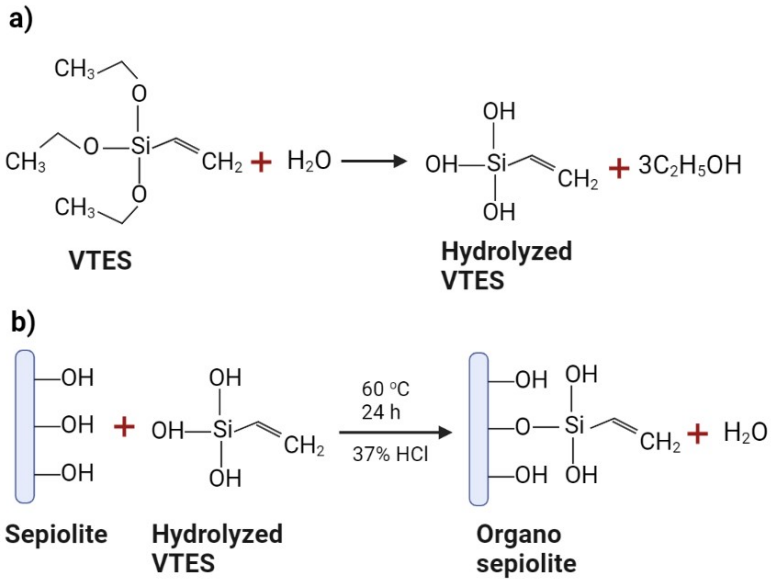


Figure 4.1: Reaction mechanism of the surface modification of sepiolite with triethoxyvinylsilane (VTES). a) Hydrolysis reaction of the organosilane and b) grafting of VTES on sepiolite.

The first part of this work aims to favor the covalent bonding or grafting of organosilanes on sepiolite surface by studying four determining reaction conditions as silane concentration, time, temperature, and

acid amount in the surface modification process. A first full factorial design was performed in order to determine the influence of the factors on the chemical grafting percentage of silane molecules on sepiolite surface, which is our response variable. Then, a second DoE is performed to find the silane concentration and HCl amount values that maximize the silane grafting. It is important to mention that both DoEs were performed around vinyltriethoxysilane (VTES) and 2-propanol used as solvent.

The amount of silane chemically bonded to the sepiolite surface provides information about the available reaction sites on the clay surface.[50] In this case, this sites corresponds to vinyl functionalities that allow the initiation and propagation of polystyrene chains on the sepiolite surface enhancing the interaction between sepiolite and polystyrene. Furthermore, during the in situ polymerization process, it is important to avoid the hydroxyl groups on sepiolite surface, as they can act as quenchers and terminate the polymerization reaction. In this way, the silane grafting percentage is an important response variable that has to be controlled for the further nanocomposite foaming process. The explanation of the silane grafting percentage estimation through thermogravimetric analysis (TGA) can be seen in section 4.1.4 of this chapter.

### 4.1.1 First DoE results

DoE 1 consisted on the full factorial design with 4 factors, two with 2 levels and the other two with 3 levels, giving a total of 36 experimental runs. The Pareto charts, shown in Figure 4.2, allow to detect the factors and interaction effects that are most important to the surface modification process. It displays the absolute values of the effects in bars, and the ones that cross a reference red line are considered statistically significant. This line for statistical importance depends on the level of significance ($\alpha$).[29] In this study a 95 % confidence level is used. As can be seen in Figure 4.2 the factors studied and the interaction between the amount of acid and time were the significant parameters in the degree of silane grafting. VTES concentration is the factor with the greatest influence on the grafting reaction.

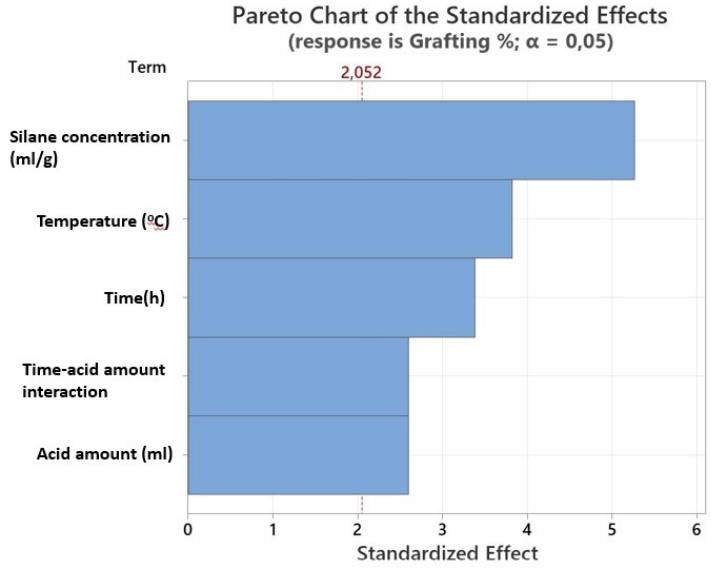


Figure 4.2: Pareto chart of the standardized effects for measured silane grafting percentage in DoE 1.

The main effect and interaction plots shows the mean response values at each level of a design,

providing insights into the magnitude and direction of the effects. The sign of the slope indicates whether the average response value increases or decreases, while the inclination indicates the strength of the effect.[51] Figure 4.3 shows the main effect plots for the factors of silane concentration, temperature, time and acid amount.

The gradual addition of VTES resulted in an increase amount of chemically grafted molecules at the surface of sepiolite, leading to a surface more covered with organosilane molecules. Within the range of 0.25 to 2.4 ml of VTES per gram of sepiolite, there is an increase of around 161 % in the silane grafting. However, it is important to consider that an excess of silane can form polycondensations between sepiolite and silane through silica bridges and form aggregations, reducing their dispersibility.[24,52] Although this effect is not considered a response variable in the design of experiments due to the complexity of quantification, it will be discussed during the preparation of the polystyrene/sepiolite nanocomposite via in-situ polymerization.

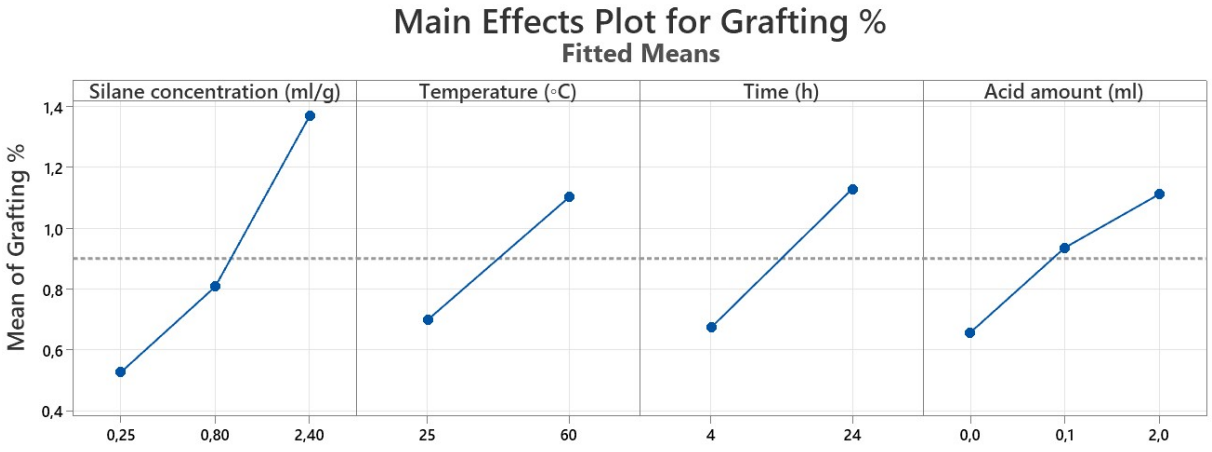


Figure 4.3: Main effect plots of the four factors studied in DoE1 for silane grafting percentage.

In the temperature case, it was found that the grafting percentage increases for the highest temperature used. By using a temperature of 60 $^{o}C$ the VTES grafting percentage rises by approximately 57.9 % in comparison when using room temperature. Previous studies have reported that temperature can accelerate the interactions between silane derivatives and silanol groups on the inorganic surface,[50] further emphasizing the significance of this factor within the studied temperature range.

In a similar way, the silane grafting percentage demonstrates an increase of around 67.9 % when the reaction time is changed from 4 to 24 hours. Longer reaction times are beneficial for the hydrolysis and condensation of VTES molecules on the silanol groups of the sepiolite surface. Regarding the amount of acid added to the reaction, it was found that the grafting percentage increases with the addition of HCl. When 0.1 ml of HCl is added to the almost neutral solution there is an increase of around 42.6 %. Meanwhile, when the amount of HCl increases from 0.1 ml to 2 ml there is an increase of 18.8 %. The addition of acid promotes hydrolysis and improves the efficiency of hydroxyl condensation with the sepiolite surface,[53] thereby enhancing the silane grafting.

The interaction between acid amount and reaction time present in Figure 4.4 shows an interesting effect. Previously, it was determined that a reaction time of 24 hours is more effective than 4 hours in increasing the amount of silane grafting. However, when using an acid amount of 2 ml, a duration of

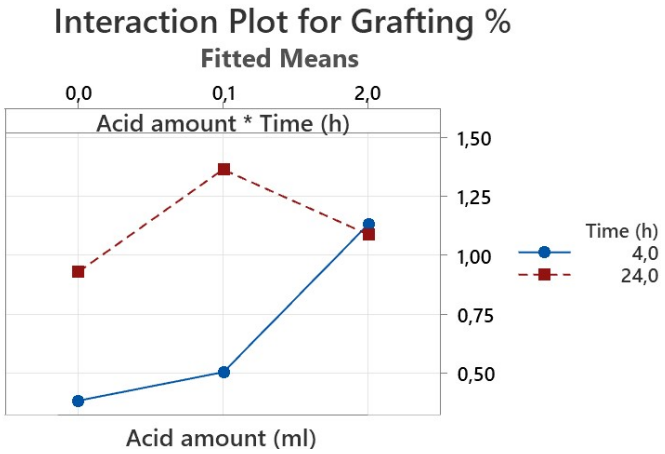


Figure 4.4: Interaction plots of pH and reaction time factors for silane grafting percentage.

4 hours is more advantageous than 24 hours. That is, for longer reaction times, using highly acidic pH values results in a lower amount of VTES molecules chemically bonded to the sepiolite surface. Previous studies on the acid activation of sepiolite have revealed that treating sepiolite with an acid leads to the destruction of the clay structure's octahedral sheet and the formation of silica.[54] Consequently, under conditions of pH 2 and a reaction time of 24 hours, the structure and composition of the sepiolite surface may undergo alterations that reduce the number of active sites available for covalent bonding with the silane molecules. Also, VTES hydrolysis and/or condensation could be diminish in presence of higher amounts of acid.

Among the conducted experimental runs, run number 25 exhibited the highest silane grafting percentage with a value of 2.76%. In this case, the experimental conditions consisted of 2.4 ml of VTES per gram of sepiolite, a temperature of 60 $^oC$, a reaction time of 24 hours and the addition of 0.1 ml of hydrochloric acid. These factor values align with the results obtained from the main effect and interaction plots, as well as with the response optimizer tool in Minitab, which identifies the combination of input variable settings that optimize the silane grafting percentage.

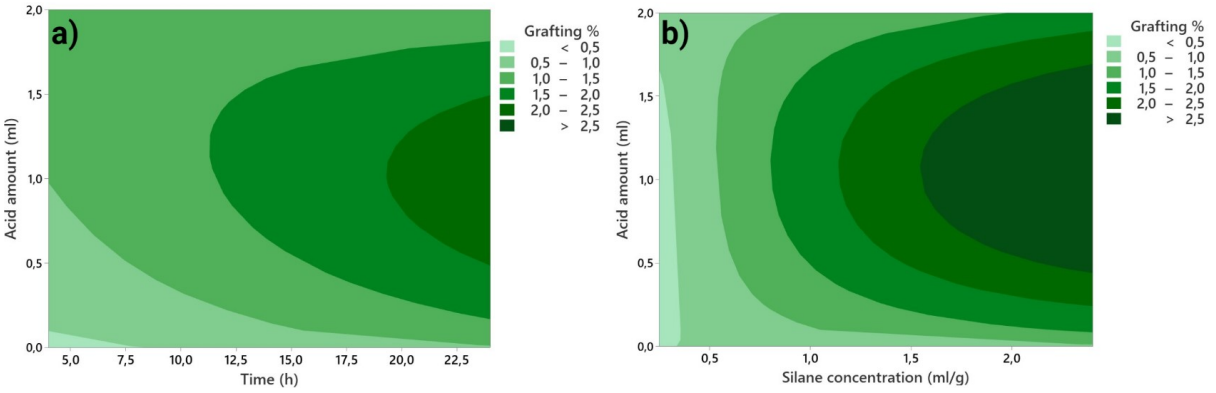


Figure 4.5: Contour plots from DoE 1 results of VTES grafting % vs a) silane concentration and acid amount, b) time and acid amount.

Contour plots provide a visual representation to explore the three-dimensional relationship between

variables in two dimensions.[55] Figure 4.5 shows silane concentration (or time) and acid amount plotted on the x and y axis, respectively, and the VTES grafting % values represented by contours while keeping constant the rest of the factors. The analysis from the previous section revealed that HCl enhance the amount of VTES molecules chemically bonded to the sepiolite surface until the addition of certain amount. This is consistent with the contour plots, the maximum grafting amount can be obtained only around the addition of 0.6 to 1.5 ml of acid.

### 4.1.2 Second DoE results

Considering the observed interaction between time and acid amount and the wide range of acid amounts ranging from 0.1 ml to 2 ml, it was decided to carry out a second DoE. So, the study aimed to determine the optimal amount of HCl for a fixed temperature and reaction time of 60 $^oC$ and 24 hours, respectively. Additionally, to determine whether the amount of silane used in the reaction reaches a saturation point in the amount of grafting, silane concentrations between 1.6 and 3.2 ml of VTES per gram of sepiolite were used. Consequently, experiments were designed using a $3^2$ full factorial design consisting of 2 factors with 3 levels each. This can be seen with the experimental run 3 of Table 6.2 in annexes, which has the same reaction conditions and exhibits a lower grafting percentage compared to the value obtained using the DoE 1 methodology (run 25 in Table 6.1 in annexes). This difference could be due to a higher interaction between HCl with the sepiolite, causing an increase in sepiolite surface reactivity before VTES is added.[54]

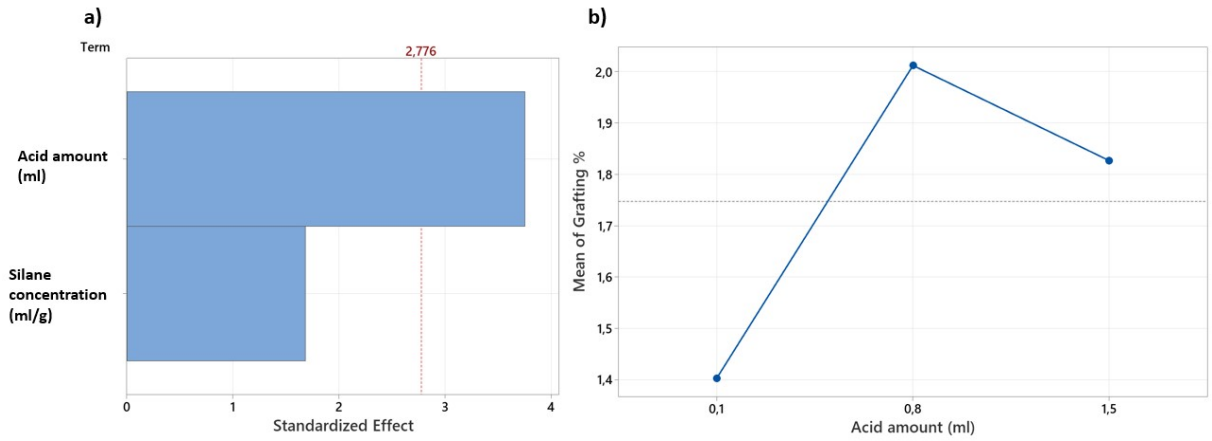


Figure 4.6: a) Pareto chart of the standardized effects for measured silane grafting percentage with B= Acid amount and b) main effect plot of acid amount factor in DoE 2.

In this case, the Pareto chart displayed in Figure 4.6 a) shows that only the acid concentration factor is considered statistically significant in the grafting reaction. Unlike the findings from DoE 1, where the silane concentration was the most significant factor. Within this range of silane concentrations, the pH of the reaction holds greater importance for VTES grafting. Table 6.2 reveals that the grafting percentage values obtained using 3.2 ml of silane per gram of sepiolite are slightly higher than the values obtained using 2.4 ml of silane per gram of sepiolite, but there is no longer a significant statistical difference as in the ones obtained at lower silane concentrations.

The main effect plot of acid factor A in Figure 4.6 b) shows a maximum in grafting at 0.8 ml.

Increasing the HCl amount from 0.1 to 0.8 ml results in an approximately 37 % enhancement in silane grafting. However, continuing to raise the acid amount from 0.8 to 1.5 ml leads to a decrease in grafting by approximately 8 %.This outcome substantiates the existence of an optimal acid amount or pH value beyond which the grafting reaction is no longer favored. As explained earlier, this could be attributed to the modification of the sepiolite composition and structure under these reaction conditions or a decrease in the efficiency of the hydrolysis and condensation of the silane molecules. So, an acid amount of 0.8 ml was chosen as the best reaction condition for the silane grating of VTES among the studied parameters.

### 4.1.3 Statistical analyses and model adequacy for grafing percentage

Analysis of variance (ANOVA) summarises the statistical analyses of the DoEs responses corresponding to VTES grafting percentage calculated from TGA. In Table 4.1 it is possible to see the associated probability values (p-values) for the factors levels and interactions of each DoE. These values measures the evidence against the null hypothesis, which implies that there is no connection between the term and the corresponding response.[56] Only p-values that are less than 0.05 allow to conclude that changes in these variables (in this case for each level) are associated with changes in the response variable. Therefore, factors and interactions that lack statistical significance can be considered as part of the error. The linear regression equation was derived by fitting the real variables at different levels for each response.[29] In all linear models, the coefficient with maximum absolute value present the highest effect on the response. In this case, in DoE 1 the maximum coefficients was found on factor A (silane concentration) with the levels correponding to 0.25 ml and 2.4 ml per gram of sepiolite, as expected from the corresponding Pareto chart.

Table 4.1 also compiles the $R^2$ values for each model. Both DoEs present a similar $R^2$ around 75%, which shows that the model fitting to the experimental data is reasonable. The obtained value could be related to experimental errors arising from small differences in reactant amounts, thermal fluctuations, presence of impurities, and reaction times. Conducting replicate measurements of the experiments can help mitigate the impact of these experimental errors. Additionally, linear regression equation are present in Table 4.1, which translate the response generation capacity of a mathematical model according to the used factorial design. Moreover, the model's adequacy was assessed through residual analysis using normal probability plots of the residuals at a 95% confidence level for grafting percentage under the conditions studied. These plots, shown in Figures 6.1 and Figure 6.2 of annexes, determine the accuracy of the model fit by examining the hypothesis of normality and equality of variance.[29] All the plots exhibit similar behaviours and indicate that the residuals closely align with the straight line.

### 4.1.4 Sepiolite thermogravimetric analysis

The quantity of grafted VTES molecules and the nature of the bonding were determined by thermal anaylisis. Figure 4.2 compares the TGA and DTG curves of pristine sepiolite and VTES, ATES and TCVS modified sepiolites used for the nanocomposites synthesis. Pristine sepiolite present four steps of degradation, which are associated with four dehydration processes in the range 50-1000 $^oC$ in good accordance with the literature.[23,57,58]

- 50-150 $^oC$: removal of zeolitic water.

Table 4.1: Coefficients and p-values for the interaction model of the responses and the general linear regression equation obtained from ANOVA.

| **Term** | **DoE 1 results** | | **Term** | **DoE 2 results** | |
|---|---|---|---|---|---|
| | **VTES grafting percentage** | | | **VTES grafting percentage** | |
| | **Coefficient** | **p-value** | | **Coefficient** | **p-value** |
| Constant | 0.8994 | 0.000 | Constant | 1.7472 | 0.000 |
| A(0.25) | -0.3752 | 0.000 | A(0.1) | -0.3438 | 0.010 |
| A(0.80) | -0.0935 | 0.278 | A(0.8) | 0.2645 | 0.030 |
| A(2.40) | 0.4687 | 0.000 | A(1.5) | 0.0794 | 0.427 |
| B(25) | -0.2021 | 0.002 | $R^2$ | 71.37 % | |
| B(60) | 0.2021 | 0.002 | | | |
| C(4) | -0.2280 | 0.001 | $R^2$ (adj.) | 61.83 % | |
| C(24) | 0.2280 | 0.001 | | | |
| D(0.0) | -0.2447 | 0.007 | **DoE 1 linear regression equation** | | |
| D(0.1) | -0.0343 | 0.688 | | | |
| D(2.0) | 0.2104 | 0.019 | | | |
| C*D(4-0) | -0.0458 | 0.592 | $\sigma_{max}$=0,8994-0,3752A(0.25)-0,0935A(0.8)+0,4687(2.4) - 0,2021B(25)+0,2021B(60)-0,2280C(4)+0,2280(24)- 0,2447D(0)+0,0343D(0.1)+0,2104D(2)-0,0458 C*D(4-0)-0,2035C*D(4-0.1)+0,2493C*D(4-2)+ 0,0458C*D(24-0)+0,2035C*D(24-0.1)-0,2493C*D(24-2) | | |
| C*D(4-0.1) | -0.2035 | 0.023 | | | |
| C*D(4-2) | 0.2493 | 0.006 | | | |
| C*D(24-0) | 0.0458 | 0.592 | | | |
| C*D(24-0.1) | 0.2035 | 0.023 | | | |
| C*D(24-2) | -0.2493 | 0.006 | | | |
| $R^2$ | 74.82 % | | **DoE 2 linear regression equation:** $\sigma_{max}$=1,7472-0,3438A(0.1)+0,2645A(0.8)+ 0,0794A(1.5) | | |
| $R^2$ (adj.) | 67.36 % | | | | |

- 150-350 $^oC$: loss of two of the four coordinated water molecules.
- 350-650 $^oC$: loss of the rest of coordinated water.
- 650-1000 $^oC$: dehydroxylation of sepiolite (loss of water related to structural OH).

In this case, pristine sepiolite undergoes a 2.15 % weight loss with a maximum temperature decomposition rate ($T_{max}$) at 92 $^oC$ during the first step. Some loosely bound zeolitic water is released from the sepiolite samples during the initial conditioning at 50 $^oC$ before the programmed heating. Half of the coordinated water in step two presents a 3.46 % weight loss with $T_{max}$ at 302 $^oC$. In the third step, the remaining coordination water undergoes a 2.82 % weight loss with $T_{max}$ at 519 $^oC$. The final step involves the dehydroxylation of sepiolite anhydride that looses its structure presents a 2.56 % weight loss with $T_{max}$ at 828 $^oC$.

In the case of modified sepiolite with organosilanes both dehydration of sepiolite and thermal degradation of the organic modifier take place on heating. DTG curves (Figure 4.7) present two additional decomposition peaks that gives evidence that volatilisation of the modifier takes place in two steps. At

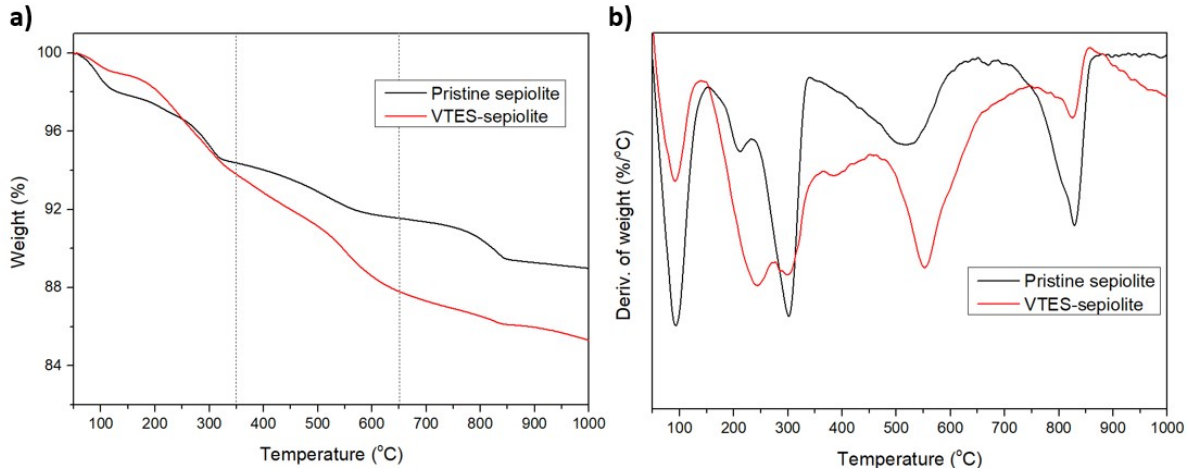


Figure 4.7: TGA and DTG curves from pristine sepioline and VTES modified sepiolite.

lower temperatures, the peak in the range of 160-280 $^oC$ corresponds to the degradation of silane non-grafted to the sepiolite structure by adsorption through hydrogen bonding or van der Waals forces.[57,58] This process partially overlaps with the first loss of coordinated water. The second additional peak in the range of 350-650 $^oC$ correspond to chemically grafted silane molecules, which overlaps with the second coordination water elimination step. The percentage of silane molecules grafted onto sepiolite was determined by analyzing the mass loss between 350 $^oC$ and 650 $^oC$, resulting in around 3.47% for VTES-Sep.

Table 4.2: Thermogravimetric analysis values of sepiolite and sepiolite modified with VTES at various temperature ranges, along with the silane grafting percentage.

| **Sample** | **Weight loss (%)** | | | | **Grafting %** |
|---|---|---|---|---|---|
| | **50-150 $^oC$** | **150-350** | **350-650** | **650-1000** | |
| **Pristine sepiolite** | 2.15 | 3.46 | 2.82 | 2.56 | - |
| **VTES-sepiolite** | 1.29 | 3.82 | 6.29 | 2.42 | 3.47 |

### 4.1.5 Sepiolite FTIR analysis

The grafting of silane molecules onto sepiolite was examined using FTIR measurements. Figure 4.8 shows the FTIR spectra of pristine sepiolite and modified sepiolite with VTES and ATES. Pristine sepiolite exhibits absorption bands at 3685 and 3552 $cm^{-1}$, which correspond to the stretching vibration of OH groups in the octahedral sheet and coordinated water molecules of sepiolite, respectively.[27,59] The absorption band at 1656 $cm^{-1}$ is associated with the H-O-H vibration of coordinated water.[59] The absorption bands at 964, 1210, and 690 $cm^{-1}$ are attributed to the Si-O vibrations. Additionally, the peak at 1002 $cm^{-1}$ is assigned to the Si-O-Si linkage in the tetrahedral sheet.[25,27,59]

In the VTES modified sepiolite, new absorption bands appear at 2978 and 1410 $cm^{-1}$, corresponding to C-H stretching vibrations in organosilanes and to in-plane deformation of vinyl $CH_2$, respectively.[27,53] Additionally, the intensity of the band at 1002 $cm^{-1}$ associated with Si-O-Si groups is significantly enhanced in sepiolite modified with VTES, indicating an increased presence of Si-O groups on the

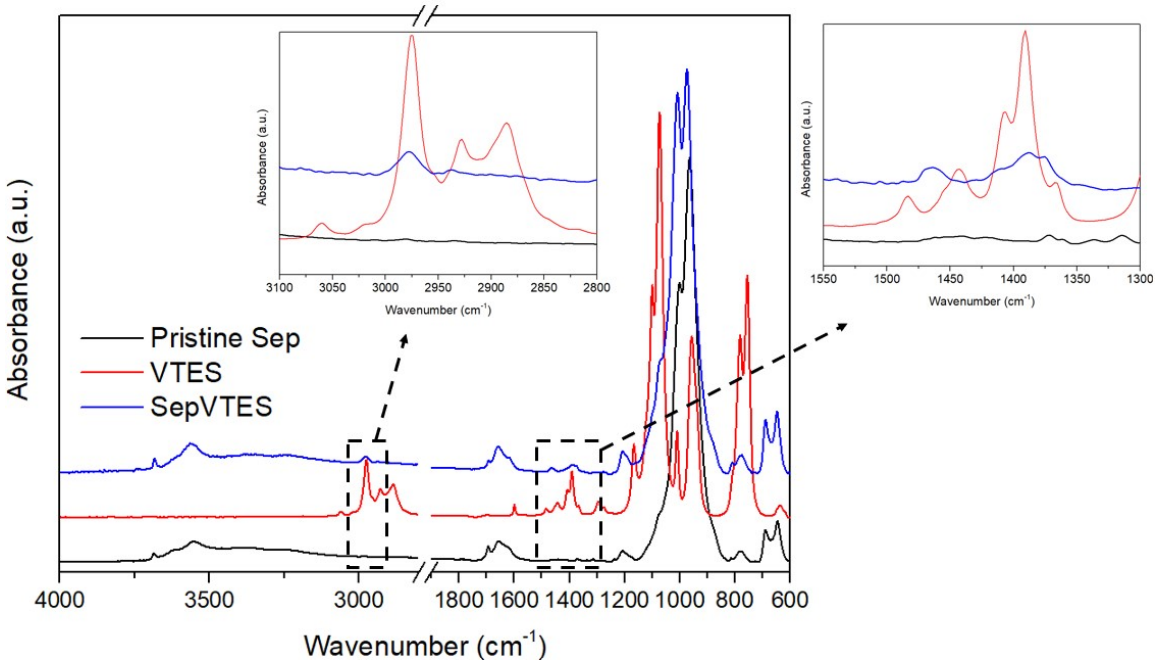


Figure 4.8: FTIR spectra of pristine sepiolite, VTES and VTES modified sepiolite in the range of 4000-600 $cm^1$.

sepiolite surface during the chemical grafting process.[59] All this information confirms the successful grafting of silane molecules onto sepiolite. It is worth noting that the presence of a low-intensity peak at 1382 $cm^{-1}$ due to the $-CH_3$ bending of ethoxy groups in VTES modified sepiolite, which suggests that not all silane molecules have undergone hydrolysis.[60]

## 4.2 Polystyrene/sepiolite nanocomposites

Prior to the synthesis of polystyrene/sepiolite nanocomposites, the dispersibility of both pristine sepiolite and silane-modified sepiolite with varying concentrations of VTES was investigated in water and styrene (4 wt. %). Photographs in Figure 4.9 shows that unmodified sepiolite present a good dispersability in water and start to sedimentate slowly after 15 minutes. As silane modification changes the surface chemistry of sepiolite and increases their hydrophobicity[11], the sample modified with 1.2 ml of VTES per gram of sepiolite present a lower dispersion stability in water. In this case, part of sepiolite particles settle down, while the remaining particles floated on the water's surface indicating that the surface modification was not homogeneously performed in this conditions. On the other hand, sepiolite modified with 3.2 ml of VTES per gram of sepiolite could not be dispersed in water and sepiolite particles remain at the top of the surface of water. The modified sepiolite particles repel or resist water, preventing them from becoming wetted. This implies that the surface of sepiolite has hydrophobic properties after the silane modification.

On the other hand, in Figure 4.10 it is possible to see that all the sepiolite samples deposited down in styrene after short times. Pristine sepiolite settled down almost immediately after mixing in the solvent. The surface modification of sepiolite using silane molecules is expected to enhance its dispersibility in weak polar or non-polar organic solvents. Although sepiolite samples grafted with VTES showed a

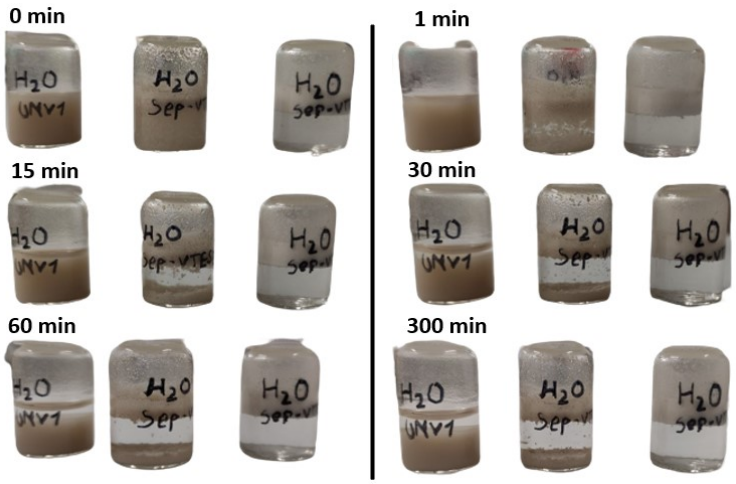


Figure 4.9: Photographs of the dispersion of unmodified sepiolite, modified with 1.2 and 3.2 ml of VTES/g of sepiolite (from left to right) in water after standing for different times.

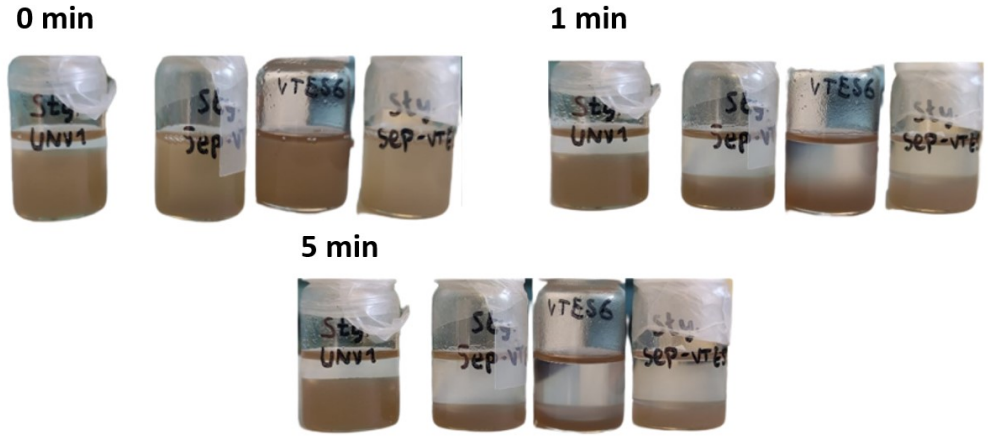


Figure 4.10: Photographs of the dispersion of unmodified sepiolite and modified with 1.2, 2.4, and 3.2 ml of VTES/g of sepiolite (from left to right) in styrene after standing for different times.

slower sedimentation rate compared to pristine sepiolite, they still lacked dispersion stability. Within around one minute, all of the VTES grafted samples also settled down, with sample modified with 2.4 ml of VTES per gram of sepiolite taking the longest to do so. The poor dispersion in styrene could be attributed to the formation of sepiolite aggregates during the surface modification process, likely due to high concentrations of silane leading to polycondensation through silica bridges.[24,52] Taking this into account and that a sonication process to enhance sepiolite dispersion in styrene it is difficult to perform, as this monomer can start to react before the addition of the organic phase in the suspension polymerization, it was decided to add the sepiolite to the aqueous phase instead of the organic phase during in suspension polymerization.

Figure 4.11 shows the in situ radical polymerization reaction of PS/sepiolite composites. When unmodified sepiolite is used in the reaction, the polystyrene and the filler are not chemically bonded, resulting in the presence of only free polystyrene chains that undergo initiation and growth through radical

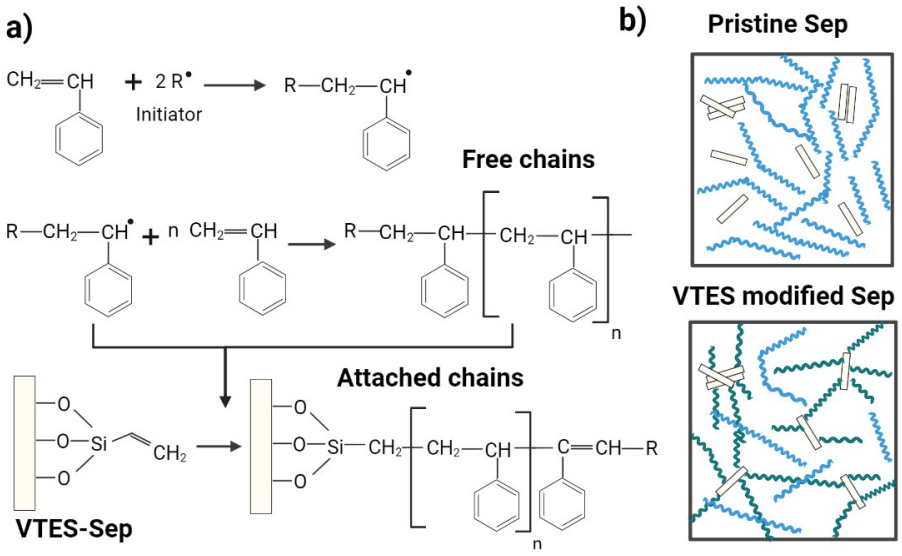


Figure 4.11: In situ radical polymerization of PS/sepiolite nanocomposites showing a) initiation and propagation of PS free chains and attached PS chains to vinyl groups on sepiolite surface. b) Schematic representation of the PS/sepiolite nanocomposites formed using unmodified and modified sepiolite.

polymerization. However, when VTES-modified sepiolites are used, in addition to free chains, polymer chains become attached to the nanofillers through the vinyl groups present on the nanofiller surface. As a result, the interaction between sepiolite and the polystyrene matrix is enhanced, which can lead to improved properties of the nanocomposite.

### 4.2.1 X-ray radiography images

X-ray radiography is employed to evaluate the dispersion and distribution of sepiolite in the polystyrene matrix at a high size scale. Figure 4.12 shows the X-ray radiography images of the different PS and PS/sepiolite composites plates prepared in this work. The darker regions within these images correspond to places in the sample where a greater amount of energy is absorbed, which depends on the density of the material. For the nanocomposites obtained using unmodified sepiolite, it is possible to observe that when 1% sepiolite is used, there is no discernible change in contrast within the image. This suggests that the sepiolite is uniformly dispersed and distributed within the matrix on this scale. However, as the sepiolite content is increased to 3% and 6%, areas with slight contrast variations become noticeable, potentially indicating a less favorable distribution of the charge but with a good dispersion.

The radiography images corresponding to the composites using VTES-modified sepiolite clearly depict the presence of sepiolite aggregates within the matrix. The presence of these aggregates primarily arise from the surface modification process, during which a high concentration of silane was employed (3.2 ml of silane per gram of sepiolite). In Figure 4.13 it is possible to observe the effects that lead to the formation of sepiolite aggregates at elevated concentrations of silane, which has been reported in the silylation of layered clays and palygorskite.[52,61] The locking effect occurs when neighboring clay layers connect and become fixed through the simultaneous condensation of silane (or silane oligomer). Additionally, the welding effect takes place as sepiolite particles becomes interconnected through polysiloxane

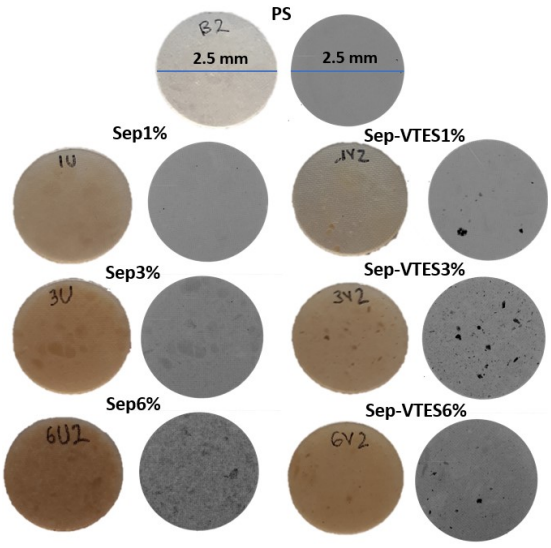


Figure 4.12: PS and PS/sepiolite composites plates and their corresponding X-ray radiography images.

bridges.[52,61]

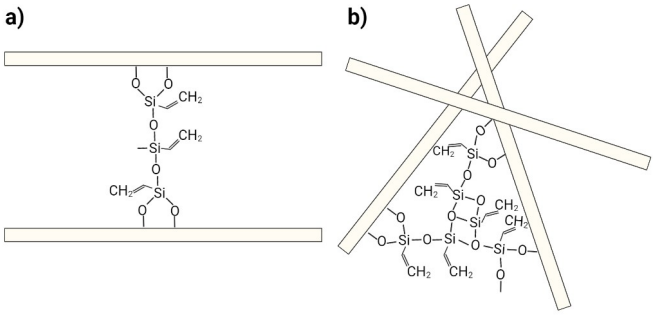


Figure 4.13: Schematic representation of the surface coupling reaction of VTES and sepiolite by a) locking effect and b) welding effect.

### 4.2.2 Molecular weight and molecular weight distribution

As the molecular weight of polymers and their distribution are closely linked to their structural and rheological properties[62], it is important to study the effect of sepiolite addition on the polystyrene matrix during the in situ polymerization process. The number-average ($M_n$) and weight-average ($M_w$) molecular weights, as well as the dispersities (Đ) of the samples, were determined by GPC technique and can be seen in Table 4.3. In the nanocomposites using unmodified sepiolite it can be seen that the $M_w$ value increases when the sepiolite amount is increased in the polymerization medium. Also, the dispersities of the pure polymer and nanocomposites with different amounts of sepiolite are similar, revealing a wide distribution of molecular weights in all cases. To understand the behavior behind GPC results, it is important to consider the molecular weight distribution of PS and nanocomposites using unmodified sepiolite present in Figure 4.14. Deconvolution of these curves can provide further insights into the characteristics of this broad molecular weight distribution.

Table 4.3: Number- and weight-average molar masses ($M_n$, $M_w$) and dispersities (Đ) obtained by GPC of the prepared polystyrene and polystyrene/sepiolite nanocomposites. The samples were recorded in $CHCl_3$ and calibrated with PS monodisperse standards.

| **Sample** | **Molar masses** | | |
|---|---|---|---|
| | $M_n$ **(g/mol)** | $M_w$ **(g/mol)** | **Đ** |
| **PS** | 69800 | 275600 | 3.9 |
| **PS-Sep1%** | 69100 | 286250 | 4.1 |
| **PS-Sep3%** | 65000 | 288450 | 4.4 |
| **PS-Sep6%** | 77300 | 332100 | 4.3 |
| **PS-SepVTES1%** | 50500 | 213600 | 4.2 |
| **PS-SepVTES3%** | 37400 | 124950 | 3.3 |
| **PS-SepVTES6%** | 54150 | 220150 | 4.1 |

The deconvolution of the curves revealed two populations of molecular weights in the neat PS and nanocomposites with unmodified sepiolite. The deconvolution of this bimodal distribution was performed using two Gaussian peaks, as seen in Figure 4.14 part b). The obtained adj. $R^2$ values above 99% in all the cases indicate a correct fitting of the peaks.

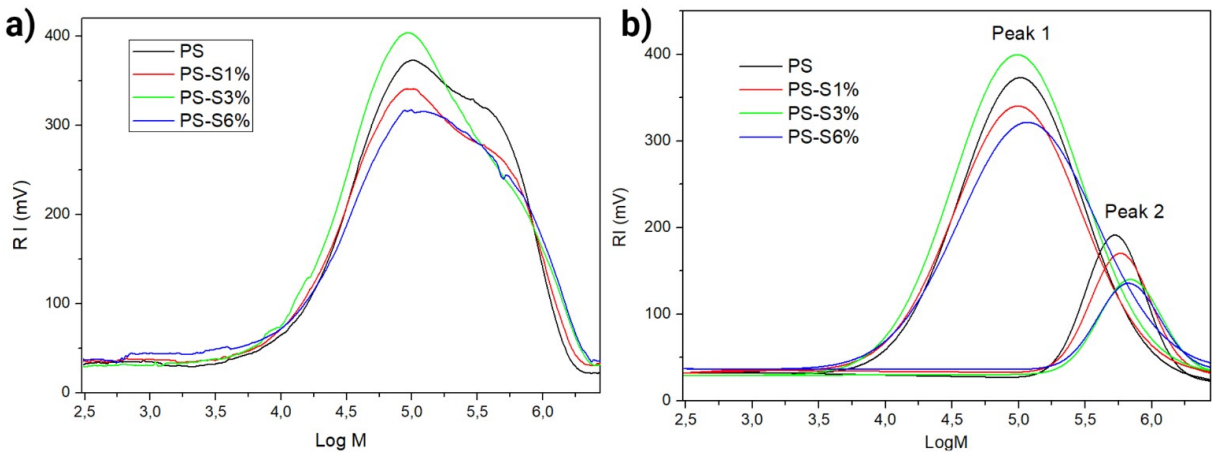


Figure 4.14: a) GPC chromatograms of neat PS and nanocomposites with unmodified sepiolite recorded in CHCl3. b) Deconvolution of chromatograms using two Gaussian functions showing a bi-modal molecular weight distribution.

Two simultaneous effects could influence the differences in molecular weight of the nanocomposites using unmodified sepiolite. The first one involves a reduction in the amount of higher molecular weight chains when introducing the filler into the polystyrene matrix and increasing its concentration. This is evident from the decrease in the maximum relative intensity of the second peak in Figure 4.14 and is supported by the data in Table 4.4. The presence of unmodified -OH groups in sepiolite is thought to play a role in this effect by increasing termination reactions during polymerization, thereby limiting the growth of polystyrene chains.[2] Therefore, the probability of growing radicals participating in irreversible reactions is enhanced by the sepiolite content.[63] Additionally, the incorporation of nanoclay, acting as an impurity in the polymerization system, increases the dispersity of the lower molecular weight peak in the

bimodal distribution from 1.7 to 2.1 with a 6 wt.% loading of sepiolite.

On the other hand, there is also an increase in molecular weight, particularly at higher sepiolite concentrations. This suggests that sepiolite may offer protection against termination reactions by exerting confinement on the steric mobility of chains, leading to the formation of higher molecular weight chains.[2] The addition of sepiolite in the reaction raises the medium's viscosity and reduces macromolecule diffusion, making it challenging for the growing chains to interact with the OH groups present in rigid sepiolite and other long chains with less fluidity compared to the monomer.[64] This effect can be seen in the increase of $M_n$ and $M_w$ values in Table 4.3 with the addition of 6% of sepiolite. An schematic representation of this effect can be seen in Figure 4.15 part b). Furthermore, previous studies have reported that nanoclay can accelerate the polymerization rate.[65,66] The presence of pendant hydroxyl groups and oxygen-containing groups in nanoclays may induce a change in polarity in the reaction medium, promoting radical activation and reducing radical recombination rates.

Table 4.4: Peak deconvolution data including maximum relative intensity and calculated $M_n$, $M_w$ and Đvalues for each peak from the GPC chromatograms of PS and PS/sepiolite nanocomposite samples.

| **Sample** | **Peak #** | **Max. relative intensity (mV)** | $M_n$ **(g/mol)** | $M_w$ **(g/mol)** | **Đ** |
|---|---|---|---|---|---|
| **PS** | 1 | 346.4 | 124559 | 206144 | 1.7 |
| | 2 | 166.7 | 551377 | 601895 | 1.1 |
| **PS-Sep1%** | 1 | 307.4 | 122985 | 230336 | 1.9 |
| | 2 | 138.3 | 609635 | 668931 | 1.1 |
| **PS-Sep3%** | 1 | 369.0 | 123623 | 250300 | 2.0 |
| | 2 | 109.3 | 731061 | 813748 | 1.1 |
| **PS-Sep6%** | 1 | 285.2 | 154744 | 319674 | 2.1 |
| | 2 | 99.5 | 707630 | 787340 | 1.1 |

During the in situ polymerization process, there is a competition between the effects mentioned before. Figure 4.15 a) shows the relationship between $M_w$ and the amount of sepiolite added in the in situ polymerization reaction. In the non-deconvoluted molecular weight distribution and the lower molecular weight peak in the deconvoluted curve, which contain smaller chains, their higher mobility facilitates interactions with the OH groups, leading to increased termination reactions. As a result, the protective effect becomes more pronounced at higher sepiolite concentrations, evident in a significant increase in $M_w$ at 6% wt. of sepiolite. On the other hand, peak 2 of the deconvoluted curve presents chains with the highest molecular weights, so the protective effect is primarily observed at low amounts of sepiolite. In this case, when 6% wt. of sepiolite is used, the $M_w$ decreases as the mobility of these chains is significantly reduced, hindering their interaction with the monomers and radicals in the medium.

The composites containing VTES modified sepiolite exhibit a decrease in $M_n$ and $M_w$ compared to the other materials, as shown in Table 4.3. This reduction in molecular weight can be attributed to the increased chain transfer reactions between the propagating chain radicals and vinyl groups, allowing the growth of polystyrene chains on sepiolite surface.[52] Another interesting effect found of using VTES modified sepiolite in the in situ polymerization was the alteration of the bimodal molecular weight distribution found in neat PS and PS/unmodified sepiolite nanocomposites into a single peak distribution

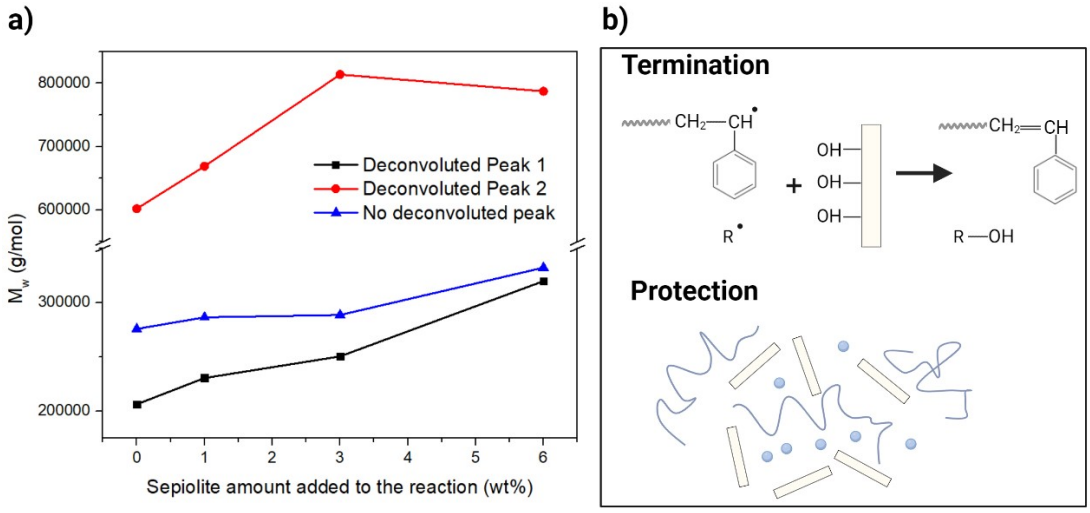


Figure 4.15: a) Impact of the amount of unmodified sepiolite added to the reaction on the weight average molecular weight $M_w$ of the nanocomposites. b) Schematic representation of the competing mechanisms of termination and protection during the in situ polymerization process.

(Figure 4.16). Additionally, an unexpected reduction in the molecular weight of the PS-SepVTES3% compound was observed. This is mainly due to the sensitivity of the in situ polymerization process to experimental parameters, which can influence the molecular weight of the polymer matrix in a polymeric compound.

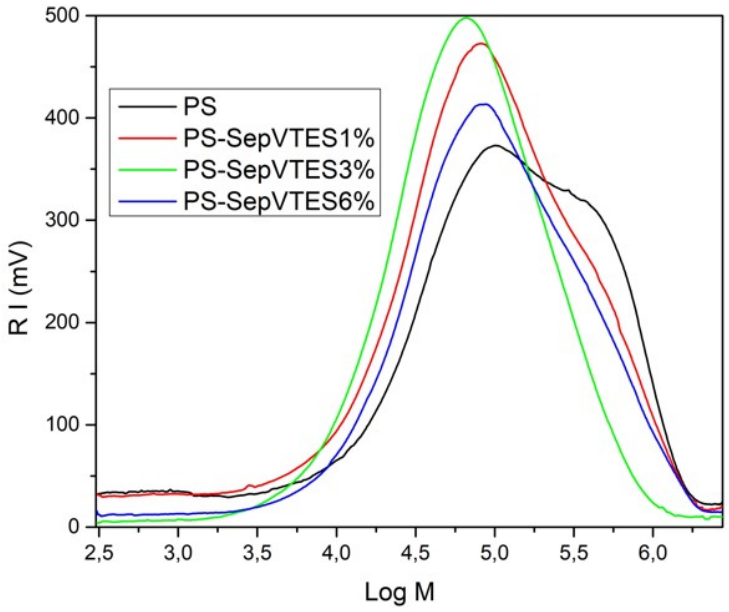


Figure 4.16: GPC chromatograms of neat PS and composites with VTES modified sepiolite.

### 4.2.3 Thermal analysis

Thermogravimetric analysis (TGA) was performed on neat PS and PS/sepiolite composites to determine the effects of sepiolite on their thermal stability and to evaluate the final clay amount in the nanocomposites. The resulting differential thermogravimetric (DTG) thermograms are shown in Figure 4.17 in the temperature window of 50 to 750 $^oC$. At temperatures below 250 $^oC$, all of the samples present an small weight loss (0.9 to 2.7 wt.%) due to humidity and residual silane molecules that were not chemically bonded to sepiolite.[63] The main degradation peak for both the synthesized PS and the different nanocomposites occurred within the temperature range of 300-500 $^oC$.

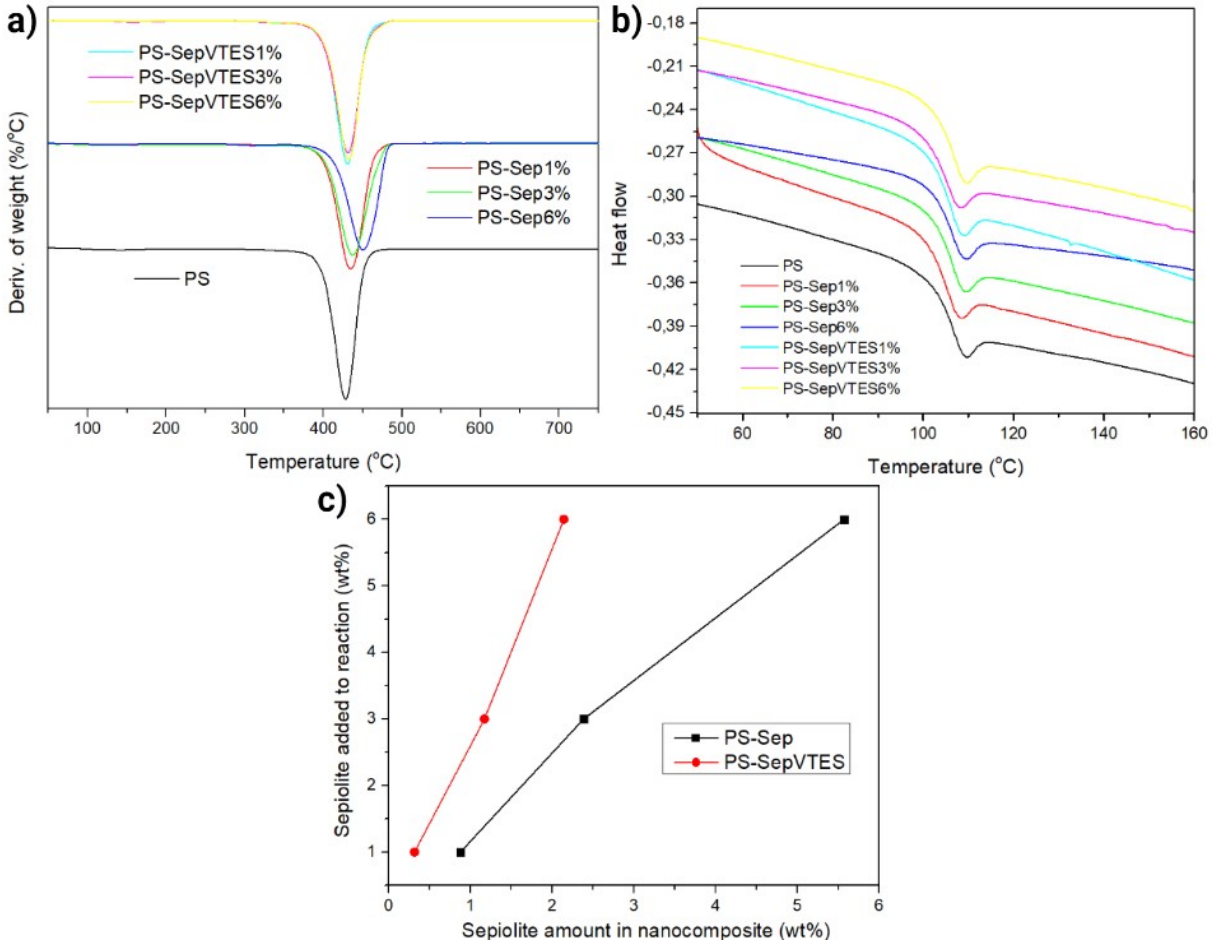


Figure 4.17: a) DTG and d) DCS curves of pure polystyrene and composites containing unmodified/unmodified sepiolites. c) Relation between sepiolite added to reaction and sepiolite final amount present in the nanocomposites.

The sepiolite content in the PS nanocomposites, both with unmodified and modified sepiolite, can be found in Table 4.5. The experimental relationship between the amount of clay added at the start of in situ polymerization and the final amount of charge remaining in the nanocomposite can be seen in Figure 4.17. When VTES-modified sepiolite was employed, a noticeable reduction in clay content was observed compared to using unmodified sepiolite. This difference can be attributed to the hydrophobic nature of VTES-modified sepiolite, which hindered its dispersion in the aqueous phase during in situ polymerization. Furthermore, the presence of large aggregates resulting from the polycondensation

between sepiolite and the high concentration of silane further impeded the interaction between the monomers in the organic phase and sepiolite. However, due to the heterogeneous nature of these samples with the presence of aggregates and the fact that only one TGA measurement was conducted, there are a significant experimental error in these values. The investigation of the final charge amount in the nanocomposite and its interaction with the matrix is crucial, as it can greatly impact the mobility of the chains, thereby influencing their rheological behavior and transition temperatures.[2,13]

Table 4.5: Calculated and extracted data from TGA/ DTG and DSC thermograms for the neat polystyrene and its nanocomposites.

| **Sample** | **TGA** | | **DSC** |
|---|---|---|---|
| | **Sepiolite amount (wt%)** | $T_{onset}$ ($^oC$) | $T_g$($^oC$) |
| **PS** | - | 428.5 | 101.8 |
| **PS-Sep1%** | 0.88 | 435.3 | 100.6 |
| **PS-Sep3%** | 2.38 | 437.8 | 101.9 |
| **PS-Sep6%** | 5.57 | 450.6 | 101.9 |
| **PS-SepVTES1%** | 0.31 | 430.6 | 101.1 |
| **PS-SepVTES3%** | 1.17 | 431.5 | 100.2 |
| **PS-SepVTES6%** | 2.14 | 432.7 | 102.1 |

The nanocomposites exhibit higher thermal stabilities compared to the neat polystyrene and rises by increasing sepiolite loading, as can be seen with the onset temperatures of thermal decomposition ($T_{onset}$) in Table 4.5. This improvement can be attributed to the superior thermal stability of the nanofillers, which act as a physical barrier against decomposition products.[65] Among the nanocomposites, those with unmodified sepiolite demonstrate the highest $T_{onset}$ values, reaching a maximum of 450.69 $^oC$ when 6% wt. of sepiolite is incorporated. This may be attributed to a better dispersion[67] and larger amount of sepiolite present in these nanocomposites in comparison with composites with VTES modified sepiolite.

To determine the glass transition temperature ($T_g$) of the samples, DSC analysis was performed, and the corresponding thermograms of pure polystyrene and its various nanocomposites are shown in Figure 4.17 b). The observed endothermic process accompanying the glass transition of the polymer could indicate the rearrangement of low molecular weight fractions with relaxed segments that were initially packed together. The obtained $T_g$ values, as presented in Table 4.5, do not exhibit significant changes in any of the cases. It would be expected that nanocompounds with populations of chains of lower molecular weight to have lower $T_g$ values, as they can reduce viscosity.[63] However, the obtained $T_g$ values do not provide conclusive evidence in this regard.

### 4.2.4 Rheology

As the rheological properties of particle-filled materials are highly responsive to their structure, rheology provides a valuable tool for evaluating the dispersion state in nanocomposites. So, shear dynamic rheology is used in this work to evaluate the dispersion of sepiolite particles in the polystyrene matrix. The incorporation of inorganic fillers, such as nanoparticles, brings about modifications in the behavior of

the polymer matrix (as an increase in viscosity at low shear rates), resulting in changes in the zero-shear viscosity, storage and loss modulus curves, cross frequency points and complex viscosity.[3,68].

In a pure polymer matrix, the storage modulus and loss modulus exhibits a typical relaxation behavior where $G' \sim \omega^2$ (slope ~ 2) and $G'' \sim \omega$ (slope ~ 1). Moreover, there is only one cross-over point between these two curves at lower frequencies. However, when particles are incorporated into the polymer matrix, this behavior is altered. Increasing the particle density, achieved by either increasing the particle amount or improving filler dispersibility, leads to proportional slopes of 1 for both the storage and loss modulus in the terminal region. As the particle density increases, G' and G" exhibit a more solid and elastic behavior, particularly at lower frequencies where G' > G". Also, a non-Newtonian power law behavior can also be observed at lower frequencies. As the particle density continues to increase and approaches the percolation density, the number of cross-over frequency points increases from 1 to 2. A further increase in particle density can result in a response where G' > G" across the entire frequency range. This solid-like response indicates a percolated arrangement of the fillers, where they come into contact with each other along the polymer matrix.[3,68] The described effects of increasing filler density in a polymer matrix can be seen in Figure 4.18.

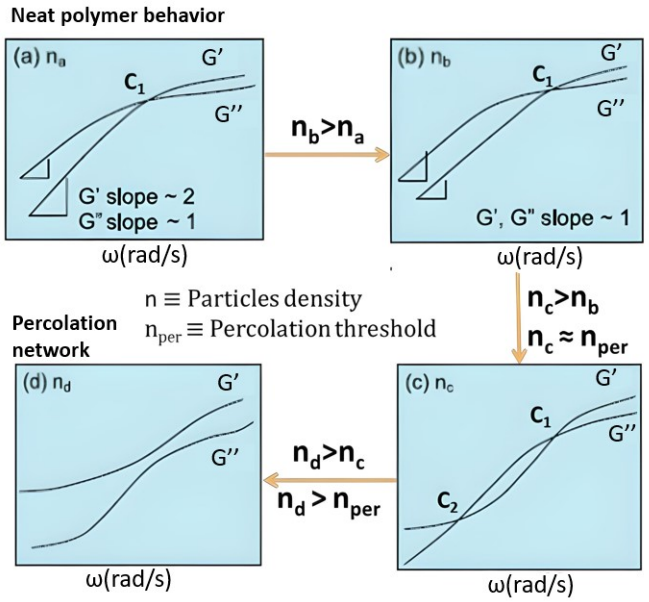


Figure 4.18: Schematic representation of the response of storage and loss modulus with the increment of particle density in a polymer matrix. Adapted from[68]

The storage modulus (G') and loss modulus (G") behavior as a function of angular frequency for neat PS and the composites with different sepiolite amounts are present in Figure 4.19. In the case of neat PS, the typical behavior of a pure polymer with only one cross-over point can be observed. The Newonian plateau could not be observed due to material degradation at low frequencies. This degradation is primarily attributed to the absence of stabilizers in the polymer plates.

In the case of PS/unmodified sepiolite nanocomposites, G' is higher than G" across the entire frequency range. This indicates a solid-like response in the molten state with the formation of a percolation network, even with a low concentration of 1 wt. % of the filler. This finding is significant because achieving

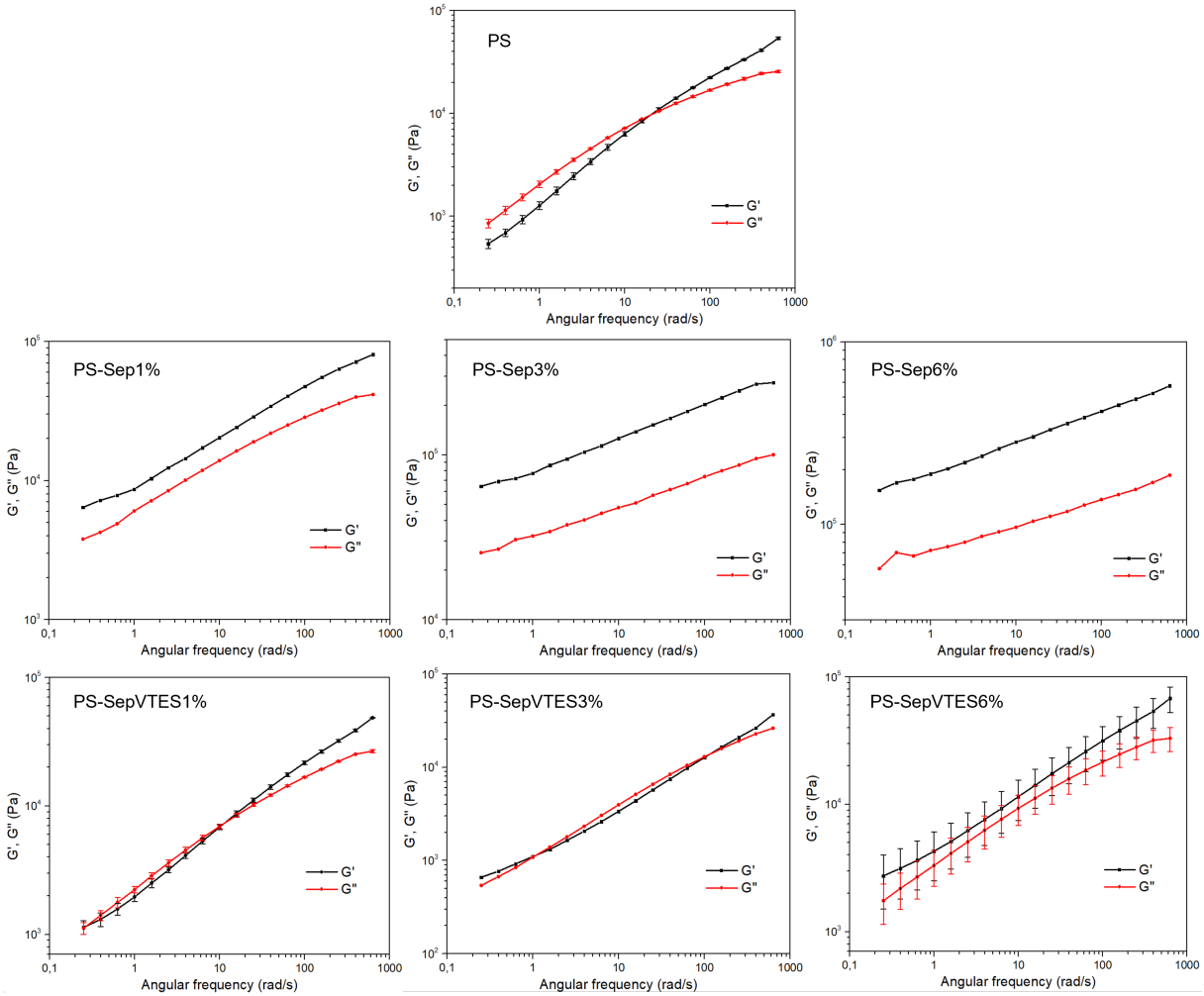


Figure 4.19: Angular frequency depdendence of the storage (G') and loss modulus (G") in the linear viscoelasticity region for neat PS and composites with unmodified and VTES modified sepiolite.

a percolation state is challenging with low particle concentrations. However, in this case, despite the low sepiolite content (1%), the particle density is high enough to form a percolation network due to the excellent dispersion achieved through in situ polymerization. Figure 4.20 illustrates a schematic representation of the percolation network, where sepiolites are interconnected and in contact with one another throughout the polymeric structure. In the work of Ballesteros et al.[39] PS/sepiolite blends prepared using the melt blending technique with a monodisperse commercial PS (INEOS, Styrolution PS153F) and the same unmodified sepiolites, achieved a percolation network using 8 wt.% of particles. This result indicates that the degree of filler dispersion in the polystyrene matrix can be significantly enhanced when employing in situ polymerization instead of melt blending technique.

On the contrary, in the compounds containing low amounts (1 and 3 wt.%) of VTES modified sepiolite, G' and G" exhibit two cut-off points. This suggests that the formation of a percolation network is close. This network is finally achieved when using 6 wt.% of VTES modified sepiolite, where G' is always greater than G". In these materials, the dispersion is poorer due to the formation of aggregates as mentioned earlier, requiring higher filler contents to achieve a percolation network. Also, it is worth

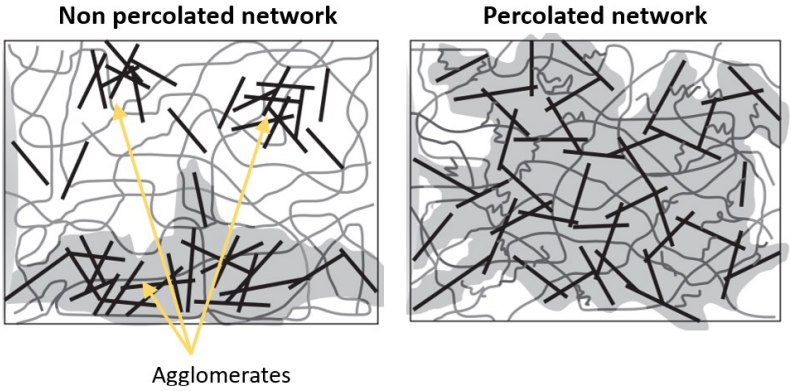


Figure 4.20: Schematic representation of sepiolite particles in a polystyrene matrix with different dispersion degrees. At the same sepiolite content, the presence of agglomerates prevent the formation of a percolated network, meanwhile a good dispersion results in the formation of a percolated network.

noting that that due to the in situ polymerization nature, the actual amount of sepiolite incorporated into the final compound is lower than the initial amount added to the reaction.

The shifting to lower frequencies of the crossover points between G' and G" curves, resulting from the addition of VTES modified sepiolite, indicates that the dominant behavior is elastic rather than viscous, as a result of the elastic properties of sepiolite.[69] This implies that the incorporation of sepiolites into a PS matrix alters the long-time relaxation behavior of the polymer by increasing the relaxation time because the nanocomposite structure creates a significant energy barrier against molecular motion during shear flow.[70]

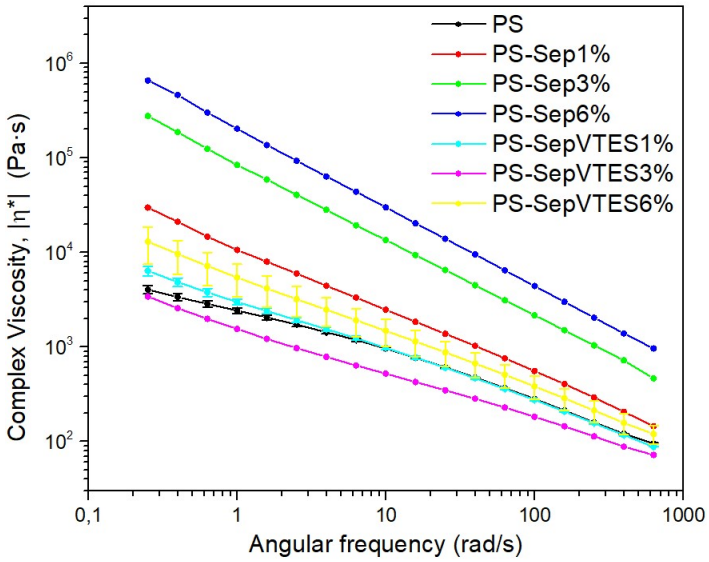


Figure 4.21: Complex viscosity versus angular frequency curves for neat PS and nanocomposites with unmodified and VTES modified sepiolite.

Figure 4.21 shows an increase in the complex viscosity ($|\eta^*|$) values of the nanocomposites containing unmodified sepiolite with respect to the neat PS. Furthermore, the viscosity of these materials increases

as the particle content increases , and the viscosity at low frequencies follows a non-Newtonian power law behavior commonly observed in polymers with fillers. Conversely, the compounds with VTES modified sepiolite consistently exhibit lower viscosities than those with unmodified sepiolite, with only the one with 6 wt. % surpassing the viscosity of the blank sample. This behavior can be attributed to the inadequate dispersion achieved in the materials with silanes. Notably, a peculiar phenomenon is observed where the compound with 3 wt.% of VTES modified sepiolite exhibits lower viscosity compared to the 1 wt.% counterpart. This observation can be explained by the previously mentioned results from GPC, where the molecular weight of this composite was found to be lower, contributing to its higher degradation.

## 4.3 PS/sepiolite foams

The foaming process of the PS and PS/sepiolite composites from circular plates samples (Figure 3.3) was performed using the gas dissolution foaming process. Figure 4.22 displays SEM images of the foams produced using neat PS and PS/modified sepiolite composites. The neat PS, obtained through suspension polymerization and featuring a bimodal molecular weight distribution, exhibits a cellular structure with an expansion ratio of 2.475, a cell size of 6.20 $\mu m$ and a cell nucleation density of $1.18x10^{10}$ nuclei/$cm^3$. The obtained foams expansion ratio values are very limited compared to other PS foams obtained from commercially available polymers (Edistir N2380) in the work of Ballesteros et al. using similar gas dissolution foaming conditions.[3] This is mainly due to the absence of a prior mixing process and a stabilizer in the foaming precursor. Also, lower $M_n$ values of the synthesized polymer led to lower expansion ratios and highly heterogeneous samples.

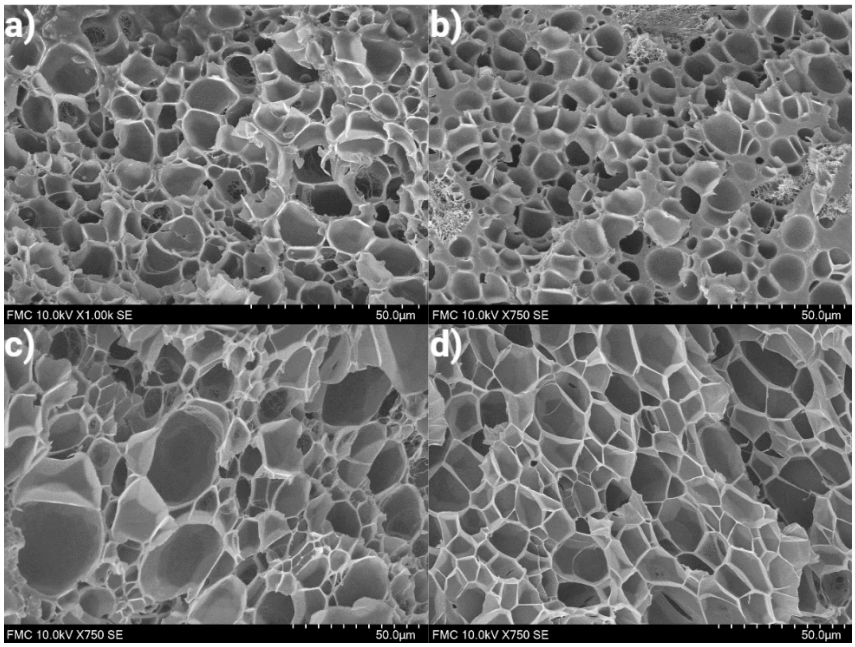


Figure 4.22: SEM micrographs of the foams samples produced from a) pure PS, b) PS-SepVTES1%, c) PS-SepVTES3% and PS-SepVTES6% composites.

Figure 4.22 displays SEM images of the cellular materials produced using pure PS and PS/modified sepiolite composites. The neat PS, obtained through suspension polymerization and featuring a bimodal

molecular weight distribution, exhibits a cellular structure with a density of 0.425 $g/cm^3$, an expansion ratio of 2.475, and a cell size of 6.20 $\mu m$. The expansion ratio of the obtained foam can be limited by the broad range of molecular weights in the polymer. The molecular weight of the polymer influences the cell structure. It is possible that regions of the polymer with shorter chains were unable to withstand the rapid expansion of the bubbles, resulting in the rupture of solid cell walls and an increase in the degeneration phenomenon.

n the case of nanocomposites with unmodified sepiolite, the presence of the filler limits the ability to generate a cellular structure in the composite. Therefore, materials with a high proportion of solid phase lacking a cellular structure are obtained. The density of these samples, shown in Table 4.6, is lower than that of the not foamed samples, primarily due to the presence of macroscopic defects.

Table 4.6: Density, relative density, expansion ratio and cell size values of the cellular materials produced by the gas dissolution foaming process.

| **Sample** | **Density** $g/cm^3$ | **Expansion ratio** | **Cell size** ($\mu m$) | **Cell nucleation density** ($nuclei/cm^3$) |
|---|---|---|---|---|
| **PS** | 0.425 ± 0.027 | 2.475 ± 0.155 | 6.20 ± 3.37 | (1.18 ± 0.12)x$10^{10}$ |
| **PS-1%Sep** | 0.679 ± 0.052 | 1.547 ± 0.119 | - | - |
| **PS-3%Sep** | 0.742 ± 0.034 | 1.416 ± 0.064 | - | - |
| **PS-6%Sep** | 0.656 ± 0.046 | 1.601 ± 0.113 | - | - |
| **PS-1%Sep-VTES** | 0.500 ± 0.013 | 2.102 ± 0.057 | 6.78 ± 3.53 | (6.75 ± 0.35)x$10^{9}$ |
| **PS-3%Sep-VTES** | 0.460 ± 0.044 | 2.286 ± 0.217 | 14.16 ± 5.21 | (8.65 ± 1.46)x$10^{8}$ |
| **PS-6%Sep-VTES** | 0.123 ± 0.001 | 8.545 ± 0.083 | 8.70 ± 4.50 | (2.19 ± 0.02)x$10^{10}$ |

On the other hand, samples produced by incorporating 1 and 3 wt% of VTES-modified sepiolite during in situ polymerization exhibit a similar expansion rate to pure PS. However, when 6 wt% of modified sepiolite is added, the expansion ratio significantly exceeds the neat PS expansion ratio, while the cell size remains similar. This indicates that silane-modified sepiolite in the composite structure substantially enhances the formation of cellular structures. This may be due to the enhanced interaction between sepiolite and the matrix, where part of the polystyrene chains are bonded to the sepiolite surface. The higher cell size and lower cell nucleation density of the sample PS-SepVTES3% could be attributed to its significantly lower molecular weight. This could lower the capacity of the material to resist gas expansion leading to a higher influence of coalescence phenomena. This behavior of the reduction in cell size and cell nucleation density for low molecular weight polymers has been reported in the work of Ballesteros et al.[3]

Two crucial parameters must be considered to produce foams with high expansion ratios and homogeneous cellular structures characterized by small cell sizes. The first one is the dispersion degree of the particles, as polymeric systems that exhibit efficient dispersion tend to have higher cell nucleation densities, resulting in smaller cell sizes.[36] Additionally, extensional rheological parameters, such as the strain hardening coefficient, play a crucial role in controlling cell degeneration mechanisms caused by coalescence.[3] This is because the viscosity of the polymer plays a crucial role as it needs to be initially low to promote the initial growth of cells, and as the foaming process progresses and the polymer experiences high extensional forces, the viscosity needs to increase to enable the solid polymer matrix to withstand

the extension without breaking.

Cell nucleation density values in Table 4.6 show an increase when 6 wt% VTES modified sepiolite is added to the in situ polymerization reaction. Despite the presence of sepiolite aggregates in the material, it was possible to significantly increase the expansion ratio while maintaining the cell size compared to pure PS foam. Therefore, optimizing the surface modification process of sepiolite is important to attain effective particle dispersion within the monomer. Such optimization is essential for producing cellular materials with enhanced properties.

# Chapter 5

# Conclusions & Outlook

Polystyrene/sepiolite nanocomposites obtained by in situ polymerization with different contents of sepiolite (1, 3 and 6 wt.%), both unmodified and surface modified with silanes groups (VTES), have been prepared and foamed. By employing the Design of Experiments (DoE) methodology, the grafting of VTES onto the sepiolite surface was maximized by controlling four determining reaction conditions: acid amount, time, temperature, and silane concentration. During the surface modification process, the formation of sepiolite aggregates occurred primarily due to the high concentration of silane, leading to polycondensation through silica bridges. Hence, optimizing the surface modification process is crucial to achieving effective dispersion of the particles within the monomer during in situ polymerization, along with the high grafting degree obtained during this work.

The in situ polymerization process is highly sensitive to experimental reaction parameters, which impact the molecular weight of the resulting nanocomposites. Under the reaction conditions employed in this study, gel permeation chromatography (GPC) measurements revealed a bimodal molecular weight distribution in both neat PS and nanocomposites with unmodified sepiolite. However, this behavior changed in the presence of VTES modified sepiolite, leading to a single peak molecular weight distribution. These variations in molecular weight have implications for the nanocomposites' final properties and the prepared foams' cellular structure.

The shear dynamic rheology measurements revealed the formation of a percolation network at 1 wt. % of unmodified sepiolite. Despite the low sepiolite content, the particle density was high enough to form a percolation network due to the excellent dispersion achieved through in situ polymerization. Additionally, the nanocomposites with unmodified sepiolite exhibited a significant increase in complex viscosity values as the particle concentration increased. TGA results indicated that the nanocomposites exhibit higher thermal stabilities than the neat polystyrene.

Although the nanocomposites with unmodified sepiolite showed improved dispersion, it was observed that the silane treatment is important for generating cellular structures in the PS/sepiolite nanocomposites. The foam with 6 wt % of VTES modified sepiolite added to the in situ polymerization reaction exhibited the highest expansion ratio and cell nucleation density, with an expansion ratio 3.5 times higher and a cell nucleation density 1.85 times higher than that of the foam produced with the neat PS. This can be attributed to the enhanced interaction between sepiolite and the polymer matrix, where part of the polystyrene chains are bonded to the sepiolite surface. However, in order to achieve foams with lower densities, it is essential to perform a mixing process and add stabilizers to the foaming precursor.

Further work is required to prevent the formation of aggregates during the surface modification process with different silane molecules and to enhance the dispersion of sepiolite in the styrene monomer during in situ polymerization. Using the least but enough amount of silane to obtain a high grafting degree makes it possible to obtain nanocomposites with a better dispersion that improves their properties. Initial steps have already been taken in this direction. An SEM image (Figure 5.1) demonstrates the reduction in cell size in a foamed sample of PS/sepiolite achieved by utilizing allyltriethoxysilane modified sepiolite. Additionally, improvements should be made to the foam precursor through a homogenization process, and the foaming process should be tailored to the properties of the nanocomposites obtained through in situ polymerization.

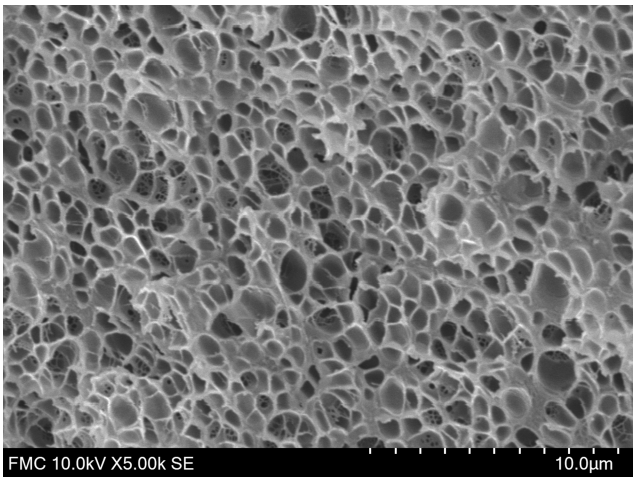


Figure 5.1: SEM micrograph foam obtained from PS and allyltriethoxysilane modified sepiolite.

# Chapter 6

# Annexes

Table 6.1: Experimental runs performed in DoE 1 and their response.

| Run | Factors | | Response |
|---|---|---|---|
| | **Silane concentration (ml/g)** | **Acid amount (ml)** | **Grafting %** |
| **1** | 2.4 | 1.5 | 1.8358 |
| **2** | 3.2 | 1.5 | 1.8738 |
| **3** | 2.4 | 0.1 | 1.552 |
| **4** | 1.6 | 0.8 | 1.6695 |
| **5** | 1.6 | 1.5 | 1.7703 |
| **6** | 1.6 | 0.1 | 1.2765 |
| **7** | 3.2 | 0.8 | 2.2672 |
| **8** | 2.4 | 0.8 | 2.0984 |
| **9** | 3.2 | 0.1 | 1.3817 |

Table 6.2: Experimental runs performed in DoE 2 and their response.

| **Run** | **Factors** | | | | **Response** |
|---|---|---|---|---|---|
| | **Silane concentration (ml/g)** | **Temperature (∘C)** | **Time (h)** | **Acid amount (ml)** | **Grafting %** |
| **1** | 2.4 | 25 | 4 | 0 | 0.40 |
| **2** | 0.8 | 25 | 24 | 2 | 0.61 |
| **3** | 0.25 | 60 | 4 | 0 | 0.48 |
| **4** | 0.25 | 60 | 4 | 0.1 | 0.21 |
| **5** | 0.25 | 25 | 24 | 2 | 0.25 |
| **6** | 0.8 | 60 | 4 | 2 | 1.01 |
| **7** | 0.8 | 25 | 4 | 2 | 0.74 |
| **8** | 0.8 | 60 | 24 | 0.1 | 1.07 |
| **9** | 0.25 | 60 | 4 | 2 | 0.75 |
| **10** | 2.4 | 25 | 4 | 0.1 | 0.45 |
| **11** | 0.25 | 60 | 24 | 2 | 0.79 |
| **12** | 0.8 | 60 | 24 | 2 | 1.52 |
| **13** | 2.4 | 60 | 24 | 0 | 1.50 |
| **14** | 0.25 | 25 | 4 | 2 | 0.99 |
| **15** | 0.8 | 60 | 4 | 0 | 0.64 |
| **16** | 2.4 | 60 | 4 | 0 | 0.61 |
| **17** | 0.8 | 25 | 24 | 0 | 0.30 |
| **18** | 0.8 | 25 | 4 | 0.1 | 0.20 |
| **19** | 2.4 | 25 | 24 | 0.1 | 1.94 |
| **20** | 0.25 | 25 | 24 | 0.1 | 0.42 |
| **21** | 0.8 | 60 | 24 | 0 | 1.33 |
| **22** | 0.25 | 60 | 24 | 0 | 0.94 |
| **23** | 2.4 | 60 | 4 | 0.1 | 1.06 |
| **24** | 2.4 | 25 | 24 | 0 | 1.03 |
| **25** | 2.4 | 60 | 24 | 0.1 | 2.76 |
| **26** | 2.4 | 25 | 24 | 2 | 1.88 |
| **27** | 0.25 | 25 | 24 | 0 | 0.47 |
| **28** | 0.25 | 25 | 4 | 0 | 0.03 |
| **29** | 2.4 | 60 | 4 | 2 | 2.24 |
| **30** | 0.25 | 25 | 4 | 0.1 | 0.31 |
| **31** | 0.8 | 25 | 4 | 0 | 0.12 |
| **32** | 2.4 | 25 | 4 | 2 | 1.05 |
| **33** | 0.25 | 60 | 24 | 0.1 | 0.65 |
| **34** | 2.4 | 60 | 24 | 2 | 1.49 |
| **35** | 0.8 | 60 | 4 | 0.1 | 0.78 |
| **36** | 0.8 | 25 | 24 | 0.1 | 1.35 |

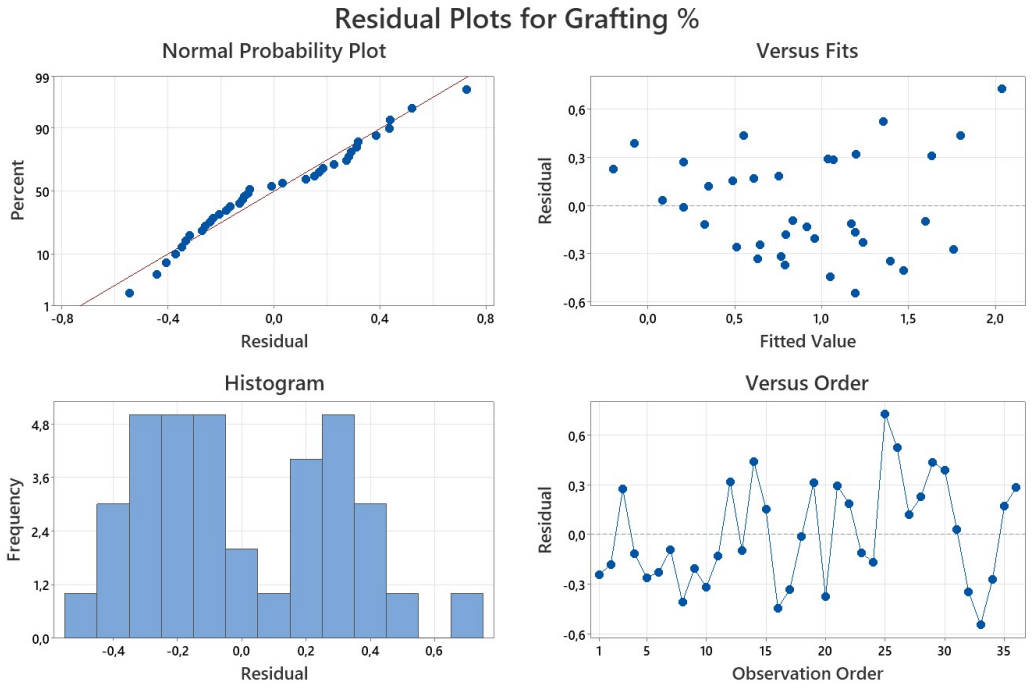


Figure 6.1: Residuals plots including normal probability, versus fits, histogram and versus order of DoE 1 response.

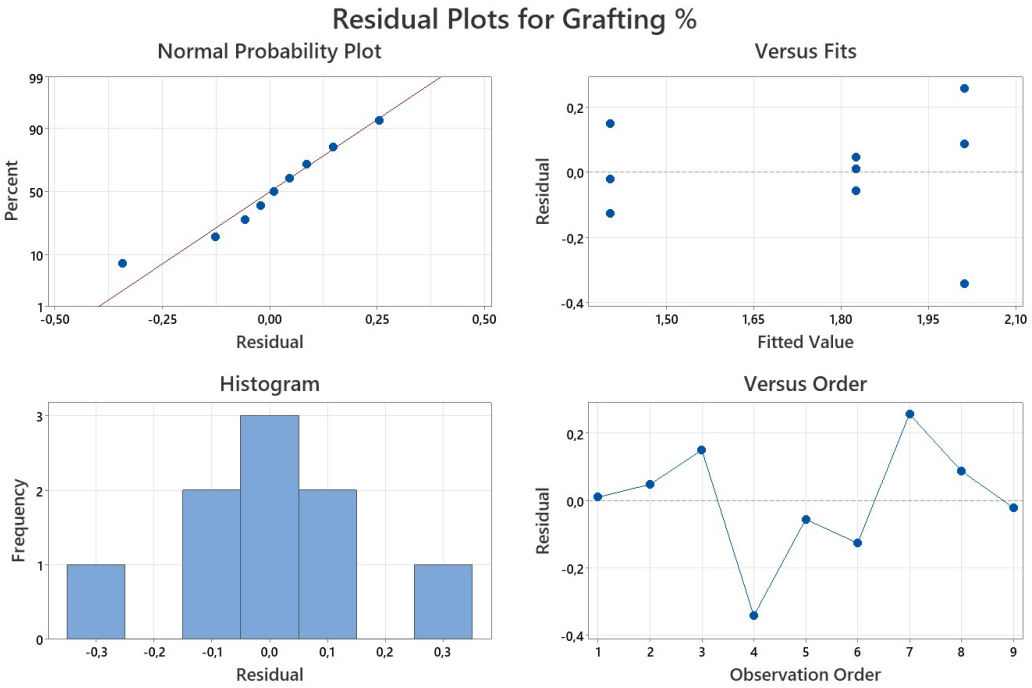


Figure 6.2: Residuals plots including normal probability, versus fits, histogram and versus order of DoE2 response.

# Bibliography


[1] Pielichowski, K.; Pielichowska, K. *Handbook of Thermal Analysis and Calorimetry*, 2nd ed.; Elsevier B.V., 2018; Vol. 6; pp 431–485.

[2] Carrero, K. C. N. Polimerización in situ de poliolefinas metalocénicas cargadas con nanosepiolita. Ph.D. thesis, Universidad de Valladolid, 2012.

[3] Ballesteros, A. Understanding the relationships between composition, process, cellular structure and properties of cellular polymers based on blends of polystyrene with inorganic and organic nucleating agents. Ph.D. thesis, 2022.

[4] Sabzi, M.; Jiang, L.; Atai, M.; Ghasemi, I. PLA/sepiolite and PLA/calcium carbonate nanocomposites: A comparison study. *Journal of applied polymer science* **2013**, *129*, 1734–1744.

[5] Laguna-Gutierrez, E.; Lopez-Gil, A.; Saiz-Arroyo, C.; Van Hooghten, R.; Moldenaers, P.; Rodriguez-Perez, M. A. Extensional rheology, cellular structure, mechanical behavior relationships in HMS PP/montmorillonite foams with similar densities. *Journal of Polymer Research* **2016**, *23*, 1–16.

[6] Tu, Z.; Wang, J.; Yu, C.; Xiao, H.; Jiang, T.; Yang, Y.; Shi, D.; Mai, Y.-W.; Li, R. K. A facile approach for preparation of polystyrene/graphene nanocomposites with ultra-low percolation threshold through an electrostatic assembly process. *Composites Science and Technology* **2016**, *134*, 49–56.

[7] Faraguna, F.; Poetschke, P.; Pionteck, J. Preparation of polystyrene nanocomposites with functionalized carbon nanotubes by melt and solution mixing: Investigation of dispersion, melt rheology, electrical and thermal properties. *Polymer* **2017**, *132*, 325–341.

[8] Krystosiak, P.; Tomaszewski, W.; Megiel, E. High-density polystyrene-grafted silver nanoparticles and their use in the preparation of nanocomposites with antibacterial properties. *Journal of colloid and interface science* **2017**, *498*, 9–21.

[9] Shin, J.-h.; Park, J.-w.; Kim, H.-j. Clay-polystyrene nanocomposite from pickering emulsion polymerization stabilized by vinylsilane-functionalized montmorillonite platelets. *Applied Clay Science* **2019**, *182*, 105288.

[10] Turhan, Y.; Doğan, M.; Alkan, M. Characterization and Some Properties of Poly(vinyl chloride)/Sepiolite Nanocomposites. *Advances in Polymer Technology* **2013**, *32*, E65–E82.

[11] Mazloom Jalali, A.; Afshar Taromi, F.; Atai, M.; Solhi, L. Effect of reaction conditions on silanisation of sepiolite nanoparticles. *Journal of Experimental Nanoscience* **2016**, *11*, 1171–1183.

[12] Martín-Alfonso, J. E.; Martín-Alfonso, M. J.; Franco, J. M. Tunable rheological-tribological performance of "green" gel-like dispersions based on sepiolite and castor oil for lubricant applications. *Applied Clay Science* **2020**, *192*, 105632.

[13] Ballesteros, A.; Laguna-Gutierrez, E.; Cimavilla-Roman, P.; Puertas, M. L.; Esteban-Cubillo, A.; Santaren, J.; Rodriguez-Perez, M. A. Influence of the dispersion of Nanoclays on the cellular structure of foams based on polystyrene. *Journal of Applied Polymer Science* **2021**, *138*.

[14] Ruiz-Hitzky, E.; Aranda, P.; Álvarez, A.; Santarén, J.; Esteban-Cubillo, A. *Developments in Clay Science*; 2011; Vol. 3; pp 393–452.

[15] Yu, Y.; Qi, S.; Zhan, J.; Wu, Z.; Yang, X.; Wu, D. Polyimide/sepiolite nanocomposite films: Preparation, morphology and properties. *Materials Research Bulletin* **2011**, *46*, 1593–1599.

[16] Tian, G.; Han, G.; Wang, F.; Liang, J. *Nanomaterials from Clay Minerals: A New Approach to Green Functional Materials*; Elsevier Inc., 2019; pp 135–201.

[17] Das, P.; Manna, S.; Behera, A. K.; Shee, M.; Basak, P.; Sharma, A. K. Current synthesis and characterization techniques for clay-based polymer nano-composites and its biomedical applications: A review. *Environmental Research* **2022**, *212*, 113534.

[18] Lynwood, C. *Polystyrene: synthesis, characteristics, and applications*; Nova publishers, 2014.

[19] Herrero, M.; Núñez, K.; Gallego, R.; Merino, J. C.; Pastor, J. M. Control of molecular weight and polydispersity in polyethylene/needle-like shaped clay nanocomposites obtained by in situ polymerization with metallocene catalysts. *European Polymer Journal* **2016**, *75*, 125–141.

[20] Nair, P. P.; George, K.; Jayakrishnan, N. Studies on mechanical behavior high impact polystyrene/vinyl clay nanocomposites: Comparison between in situ polymerization and melt mixing. *Polymer Composites* **2017**, *38*, 68–76.

[21] Kausar, A.; Rafique, I.; Muhammad, B. Aerospace application of polymer nanocomposite with carbon nanotube, graphite, graphene oxide, and nanoclay. *Polymer-Plastics Technology and Engineering* **2017**, *56*, 1438–1456.

[22] Aziz, T.; Ullah, A.; Fan, H.; Jamil, M. I.; Khan, F. U.; Ullah, R.; Iqbal, M.; Ali, A.; Ullah, B. Recent Progress in Silane Coupling Agent with Its Emerging Applications. *Journal of Polymers and the Environment* **2021**, *29*, 3427–3443.

[23] Volle, N.; Giulieri, F.; Burr, A.; Pagnotta, S.; Chaze, A. M. Controlled interactions between silanol groups at the surface of sepiolite and an acrylate matrix: Consequences on the thermal and mechanical properties. *Materials Chemistry and Physics* **2012**, *134*, 417–424.

[24] García, N.; Guzm, J.; Benito, E.; Esteban-cubillo, A.; Aguilar, E.; Santar, J.; Tiemblo, P. Surface Modification of Sepiolite in Aqueous Gels by Using Methoxysilanes and Its Impact on the Nanofiber Dispersion Ability. **2011**, 3952–3959.

[25] Rehman, S. U.; Javaid, S.; Shahid, M.; Gul, I. H.; Rashid, B.; Szczepanski, C. R.; Naveed, M.; Curley, S. J. Polystyrene-Sepiolite Clay Nanocomposites with Enhanced Mechanical and Thermal Properties. *Polymers* **2022**, *14*, 1–15.

[26] Masood, F.; Haider, H.; Yasin, T. Sepiolite / poly-3-hydroxyoctanoate nanocomposites: Effect of clay content on physical and biodegradation properties. *Applied Clay Science* **2019**, *175*, 130–138.

[27] Ajmal, A. W.; Masood, F.; Yasin, T. Influence of sepiolite on thermal, mechanical and biodegradation properties of poly-3-hydroxybutyrate-co-3-hydroxyvalerate nanocomposites. *Applied Clay Science* **2018**, *156*, 11–19.

[28] Whitford, W. G.; Lundgren, M.; Fairbank, A. *Biopharmaceutical Processing: Development, Design, and Implementation of Manufacturing Processes*; Elsevier Ltd., 2018; pp 147–162.

[29] Nuñez Carrero, K. C.; Alonso Pastor, L. E.; Hernández Santana, M.; María Pastor, J. Design of self-healing styrene-butadiene rubber compounds with ground tire rubber-based reinforcing additives by means of DoE methodology. *Materials and Design* **2022**, *221*.

[30] Cruz-Aguilar, A.; Navarro-Rodríguez, D.; Pérez-Camacho, O.; Fernández-Tavizón, S.; Gallardo-Vega, C. A.; García-Zamora, M.; Barriga-Castro, E. D. High-density polyethylene/graphene oxide nanocomposites prepared via in situ polymerization: Morphology, thermal, and electrical properties. *Materials Today Communications* **2018**, *16*, 232–241.

[31] Taimur, S.; ul Hassan, M. I.; Yasin, T.; Ali, S. W. Synthesis of modified sepiolite-g-polystyrene sulfonic acid nanohybrids by radiation induced graft polymerization. *Radiation Physics and Chemistry* **2018**, *148*, 19–24.

[32] Taimur, S.; Yasin, T.; Bibi, S. Synthesis and Characterization of Polystyrene Grafted Nanohybrids by Graft Polymerization. *Proceedings of the 2nd International Conference of Theoretical and Applied Nanoscience and Nanotechnology (TANN'18)* **2018**, 1–9.

[33] Fernández-García, L.; Pecharromán, C.; Esteban-Cubillo, A.; Tiemblo, P.; García, N.; Menéndez, J. L. Magneto-optical Faraday activity in transparent FeCo-sepiolite/polystyrene nanocomposites. *Journal of Nanoparticle Research* **2013**, *15*.

[34] Ruiz-Herrero, J. L.; Estravis, S.; Rodríguez-Perez, M. A. *Kirk-Othmer Encyclopedia of Chemical Technology*; 2017; pp 1–39.

[35] González, E. L. Analysis of the composition-structure-properties relationship of open-cell polyolefin-based foams with tailored levels of gas-phase tortuosity. Ph.D. thesis, Universidad de Valladolid, 2019.

[36] Ballesteros, A.; Laguna-Gutierrez, E.; Puertas, M. L.; Esteban-Cubillo, A.; Santaren, J.; Rodriguez-Perez, M. A. Polystyrene/sepiolites nanocomposite foams: Relationship between composition, particle dispersion, extensional rheology, and cellular structure. *Materials Today Communications* **2021**, *29*, 102850.

[37] Santiago-Calvo, M.; Tirado-Mediavilla, J.; Rauhe, J. C.; Jensen, L. R.; Ruiz-Herrero, J. L.; Villafañe, F.; Rodríguez-Pérez, M. Á. Evaluation of the thermal conductivity and mechanical properties of water blown polyurethane rigid foams reinforced with carbon nanofibers. *European Polymer Journal* **2018**, *108*, 98–106.

[38] Santaren, J.; Alvarez, A.; Esteban-Cubillo, A.; Notario, B.; Velasco, D.; Rodrıguez-Perez, M. Improving the cellular structure and thermal conductivity of PS foams by using sepiolites. 2012.

[39] Ballesteros, A.; Laguna-Gutierrez, E.; Cimavilla-Roman, P.; Puertas, M. L.; Esteban-Cubillo, A.; Santaren, J.; Rodriguez-Perez, M. A. Influence of the dispersion of Nanoclays on the cellular structure of foams based on polystyrene. *Journal of Applied Polymer Science* **2021**, *138*, 51373.

[40] Tamarit, S. P. Structural characterization of solid cellular polymers by x-ray tomography and light scattering. Ph.D. thesis, Universidad de Valladolid, 2019.

[41] Costeux, S.; Khan, I.; Bunker, S. P.; Jeon, H. K. Experimental study and modeling of nanofoams formation from single phase acrylic copolymers. *Journal of Cellular Plastics* **2015**, *51*, 197–221.

[42] Rajisha, K.; Deepa, B.; Pothan, L.; Thomas, S. Thermomechanical and spectroscopic characterization of natural fibre composites. *Interface engineering of natural fibre composites for maximum performance* **2011**, 241–274.

[43] Daéid, N. In *Encyclopedia of Analytical Science (Second Edition)*, second edition ed.; Worsfold, P., Townshend, A., Poole, C., Eds.; Elsevier: Oxford, 2005; pp 471–480.

[44] Malkoch, M.; Malmström, E.; Nyström, A. In *Polymer Science: A Comprehensive Reference*; Matyjaszewski, K., Möller, M., Eds.; Elsevier: Amsterdam, 2012; pp 113–176.

[45] Dealy, J. M.; Wang, J. *Melt rheology and its applications in the plastics industry*; Springer Science & Business Media, 2013.

[46] Torró-Palau, A.; Fernández-García, J. C.; Orgilés-Barceló, A. C.; Pastor-Blas, M. M.; Martín-Martínez, J. Structural modification of sepiolite (natural magnesium silicate) by thermal treatment: effect on the properties of polyurethane adhesives. *International journal of adhesion and adhesives* **1997**, *17*, 111–119.

[47] Puente Torres, J.; Crespo Sariol, H.; Yperman, J.; Brito Sauvanell, Á.; Carleer, R.; Navarro Campa, J. A novel X-ray radiography approach for the characterization of granular activated carbons used in the rum production. *Journal of Analytical Science and technology* **2018**, *9*, 1–15.

[48] Santiago-Calvo, M.; Pérez-Tamarit, S.; Cimavilla-Román, P.; Blasco, V.; Ruiz, C.; París, R.; Villafañe, F.; Rodríguez-Pérez, M. Á. X-ray radioscopy validation of a polyol functionalized with graphene oxide for producing rigid polyurethane foams with improved cellular structures. *European Polymer Journal* **2019**, *118*, 404–411.

[49] Omidi, M.; Fatehinya, A.; Farahani, M.; Akbari, Z.; Shahmoradi, S.; Yazdian, F.; Tahriri, M.; Moharamzadeh, K.; Tayebi, L.; Vashaee, D. *Biomaterials for oral and dental tissue engineering*; Elsevier, 2017; pp 97–115.

[50] Altaf, F.; Batool, R.; Ahmad, M. A.; Raza, R.; Khan, M. A.; Abbas, G. Novel vinyl-modified sepiolite-based polymer nanocomposites: synthesis and characterization. *Iranian Polymer Journal (English Edition)* **2018**, *27*, 413–422.

[51] Antony, J. *Design of Experiments for Engineers and Scientists*, second edition ed.; Elsevier Ltd, 2014; pp 33–50.

[52] Liu, P.; Wang, H.; Pan, C. Surface organo-functionalization of palygorskite nanorods with $\gamma$-mercaptopropyltrimethoxysilane. *Applied Clay Science* **2018**, *159*, 37–41.

[53] Hou, Z.; Zhou, D.; Chen, Q.; Xin, Z. Effect of Different Silane Coupling Agents In-Situ Modified Sepiolite on the Structure and Properties of Natural Rubber Composites Prepared by Latex Compounding Method. *Polymers* **2023**, *15*.

[54] Novel anhydrous unfolded structure by heating of acid pre-treated sepiolite. *Applied Clay Science* **2007**, *36*, 245–255.

[55] Nagarajan, V.; Mohanty, A. K.; Misra, M. Reactive compatibilization of poly trimethylene terephthalate (PTT) and polylactic acid (PLA) using terpolymer: Factorial design optimization of mechanical properties. *Materials & Design* **2016**, *110*, 581–591.

[56] Minitab, Coefficients table for Analyze Factorial Design. `https://support.minitab.com/en-us/minitab/21/help-and-how-to/statistical-modeling/doe/how-to/factorial/analyze-factorial-design/interpret-the-results/all-statistics-and-graphs/coefficients-table/`, Accessed = 19/6/2023.

[57] Basurto, F. C.; García-López, D.; Villarreal-Bastardo, N.; Merino, J. C.; Pastor, J. M. Nanocomposites of ABS and sepiolite: Study of different clay modification processes. *Composites Part B: Engineering* **2012**, *43*, 2222–2229.

[58] Tartaglione, G.; Tabuani, D.; Camino, G. Thermal and morphological characterisation of organically modified sepiolite. *Microporous and Mesoporous Materials* **2008**, *107*, 161–168.

[59] Lu, P.; Xu, J.; Liu, K. Preparation and Properties of Unsaturated Polyester Nanocomposites Based on Silylated Sepiolite Nanofibers. 2010,

[60] Lopez, J. F.; Pelaez, G. J.; Perez, L. D. Monitoring the formation of polystyrene/silica nanocomposites from vinyl triethoxysilane containing copolymers. *Colloid and Polymer Science* **2013**, *291*, 1143–1153.

[61] Tao, Q.; He, H.; Li, T.; Frost, R. L.; Zhang, D.; He, Z. Tailoring surface properties and structure of layered double hydroxides using silanes with different number of functional groups. *Journal of Solid State Chemistry* **2014**, *213*, 176–181.

[62] Gentekos, D. T.; Sifri, R. J.; Fors, B. P. Controlling polymer properties through the shape of the molecular-weight distribution. *Nature Reviews Materials* **2019**, *4*, 761–774.

[63] Khezri, K.; Roghani-Mamaqani, H. Effect of MCM-41 nanoparticles on ARGET ATRP of styrene: Investigating thermal properties. *Journal of Composite Materials* **2015**, *49*, 1525–1535.

[64] Salami-Kalajahi, M.; Haddadi-Asl, V.; Rahimi-Razin, S.; Behboodi-Sadabad, F.; Najafi, M.; Roghani-Mamaqani, H. A study on the properties of PMMA/silica nanocomposites prepared via RAFT polymerization. *Journal of Polymer Research* **2012**, *19*, 1–11.

[65] Roghani-Mamaqani, H.; Haddadi-Asl, V.; Najafi, M.; Salami-Kalajahi, M.; Najafi, M.; Salami-Kalajahi, M. Preparation of tailor-made polystyrene nanocomposite with mixed clay-anchored and free chains via atom transfer radical polymerization. *AIChE Journal* **2011**, *57*, 1873–1881.

[66] Datta, H.; Singha, N. K.; Bhowmick, A. K. Structure and properties of tailor-made poly (ethyl acrylate)/clay nanocomposites prepared by in situ atom transfer radical polymerization. *Journal of applied polymer science* **2008**, *108*, 2398–2407.

[67] Salami-Kalajahi, M.; Haddadi-Asl, V.; Rahimi-Razin, S.; Behboodi-Sadabad, F.; Najafi, M.; Roghani-Mamaqani, H. A study on the properties of PMMA/silica nanocomposites prepared via RAFT polymerization. *Journal of Polymer Research* **2012**, *19*.

[68] Laguna-Gutierrez, E. Understanding the Foamability of Complex Polymeric systems by Using Extensional Rheology. 2016. Ph.D. thesis, PhD Thesis, University of Valladolid, Spain. 346.

[69] Raji, M.; Mekhzoum, M. E. M.; Qaiss, A. e. K.; Bouhfid, R. Nanoclay modification and functionalization for nanocomposites development: effect on the structural, morphological, mechanical and rheological properties. *Nanoclay Reinforced Polymer Composites: Nanocomposites and Bionanocomposites* **2016**, 1–34.

[70] Kotsilkova, R. Rheology–structure relationship of polymer/layered silicate hybrids. *Mechanics of Time-Dependent Materials* **2002**, *6*, 283–300.